Received: 16 August 2023 | Revised: 29 February 2024 | Accepted: 8 March 2024

DOI: 10.1111/andr.13636

ANDROLOGY WILEY

ORIGINAL ARTICLE

Phosphoproteomic analysis of the adaption of epididymal epithelial cells to corticosterone challenge

David A. Skerrett-Byrne[1,2] | Simone J. Stanger[1,2] | Natalie A. Trigg[1,2] | Amanda L. Anderson[1,2] | Petra Sipilä[3] | Ilana R. Bernstein[1,2] | Tessa Lord[1,2] | John E. Schjenken[1,2] | Heather C. Murray[4,5] | Nicole M. Verrills[4,5] | Matthew D. Dun[4,5] | Terence Y. Pang[6,7] | Brett Nixon[1,2]

[1]Priority Research Centre for Reproductive Science, School of Environmental and Life Sciences, College of Engineering, Science and Environment, The University of Newcastle, Callaghan, NSW, Australia

[2]Infertility and Reproduction Research Program, Hunter Medical Research Institute, New Lambton Heights, New Lambton, NSW, Australia

[3]Institute of Biomedicine, Research Centre for Integrative Physiology and Pharmacology, and Turku Center for Disease Modeling, University of Turku, Turku, Finland

[4]School of Biomedical Sciences and Pharmacy, College of Health, Medicine and Wellbeing, University of Newcastle, Callaghan, NSW, Australia

[5]Precision Medicine Research Program, Hunter Medical Research Institute, New Lambton Heights, New Lambton, NSW, Australia

[6]The Florey Institute of Neuroscience and Mental Health, University of Melbourne, Melbourne, VIC, Australia

[7]Department of Anatomy and Neuroscience, University of Melbourne, Melbourne, VIC, Australia

Correspondence
Brett Nixon, School of Environmental and Life Sciences, College of Engineering, Science and Environment, The University of Newcastle, University Drive, Callaghan, NSW, 2308, Australia.
Email: brett.nixon@newcastle.edu.au

Funding information
National Health and Medical Research Council (NHMRC), Grant/Award Numbers: APP1147932, APP1154837, APP1173892; ChadTough Foundation

Abstract

Background: The epididymis has long been of interest owing to its role in promoting the functional maturation of the male germline. More recent evidence has also implicated the epididymis as an important sensory tissue responsible for remodeling of the sperm epigenome, both under physiological conditions and in response to diverse forms of environmental stress. Despite this knowledge, the intricacies of the molecular pathways involved in regulating the adaptation of epididymal tissue to paternal stressors remains to be fully resolved.

Objective: The overall objective of this study was to investigate the direct impact of corticosterone challenge on a tractable epididymal epithelial cell line (i.e., mECap18 cells), in terms of driving adaptation of the cellular proteome and phosphoproteome signaling networks.

Materials and methods: The newly developed phosphoproteomic platform EasyPhos coupled with sequencing via an Orbitrap Exploris 480 mass spectrometer, was applied to survey global changes in the mECap18 cell (phospho)proteome resulting from subchronic (10-day) corticosterone challenge.

Results: The imposed corticosterone exposure regimen elicited relatively subtle modifications of the global mECap18 proteome (i.e., only 73 out of 4171 [~1.8%] proteins displayed altered abundance). By contrast, ~15% of the mECap18 phosphoproteome

was substantially altered following corticosterone challenge. In silico analysis of the corresponding parent proteins revealed an activation of pathways linked to DNA damage repair and oxidative stress responses as well as a reciprocal inhibition of pathways associated with organismal death. Corticosterone challenge also induced the phosphorylation of several proteins linked to the biogenesis of microRNAs. Accordingly, orthogonal validation strategies confirmed an increase in DNA damage, which was ameliorated upon selective kinase inhibition, and an altered abundance profile of a subset of microRNAs in corticosterone-treated cells.

Conclusions: Together, these data confirm that epididymal epithelial cells are reactive to corticosterone challenge, and that their response is tightly coupled to the opposing action of cellular kinases and phosphatases.

KEYWORDS
cellular signaling, corticosterone, DNA damage, epididymis, phosphoproteomics, proteomics, sperm maturation, stress response

1 | INTRODUCTION

The epididymis is an important component of the male extratesticular reproductive system that has long been of interest owing to its dual roles in promoting the functional maturation of the male germline as well as the creation of a sperm storage reservoir.[1–8] Indeed, it is during their descent through the proximal epididymis that spermatozoa gain the potential to engage in productive interactions with an ovum as well as display the progressive motility characteristics needed to negotiate the female reproductive tract and deliver them to the site of fertilization.[8] In the absence of de novo transcriptional and translational activity, such functional transformation of the sperm cell is widely held to be driven by exposure to the complex epididymal intraluminal milieu, which itself is created by the combined secretory and absorptive capacity of the lining epithelium.[9,10] In this context, a focus for much of the research on epididymal function has been the highly regionalized production of proteins by the epididymal epithelium, which, after release to the lumen, facilitate sequential remodeling of the sperm proteome through either direct uptake or indirect means such as proteolytic processing or modification of intrinsic sperm proteins.[11–16] The scale of such changes has recently been alluded to in proteomic studies applying high-resolution quantitative mass spectrometry[17,18]; approaches that have identified in excess of 6000 mouse sperm proteins and revealed the selective loss and gain of several hundred of these proteins during epididymal transit.[18] Notwithstanding the importance of these data in confirming that mature spermatozoa carry a discrete proteomic signature that readily discriminates them from their immature counterparts, emerging evidence indicates that these changes are accompanied by substantial recasting of other molecular elements of the maturing spermatozoon.[8]

In particular, there is now compelling evidence that the sperm payload of small non-coding RNA species (sncRNAs) is substantially altered during passage of these cells through the epididymis.[19–25] Akin to their protein counterparts,[26,27] such changes appear to be mediated, at least in part, via a novel form of soma-germline communication involving trafficking via extracellular vesicles released by the epididymal epithelium as opposed to an intrinsic biogenesis program.[24,25,28] These findings have taken on added significance with the recognition that, far beyond being passive markers of sperm development, sperm-borne sncRNAs act as major conduits of epigenetic information.[24,29] Indeed, along with the paternal genome, sperm sncRNAs are delivered to the oocyte at the moment of fertilization whereupon they influence the pre-implantation gene expression program within the early embryo.[19,20] In addition to physiological regulation, there is also mounting evidence that sperm sncRNA profiles are altered in response to a variety of environmental and lifestyle factors; changes that can have potentially profound implications for downstream embryo and/or offspring development.[30–34] As the list of paternal stressors capable of eliciting transgenerational responses continues to grow, so too has interest in the timing and mechanistic basis by which the autonomic and sympathetic adaptations in a stressed animal influence the epigenetic cargo within the male germline.[29,33]

In seeking to address these questions, our group has previously modeled generalized stress by investigating the transgenerational effects of a chronic 28-day treatment of male mice with low-dose corticosterone prior to mating. This study revealed sex-specific alterations to anxiety and depression-related behaviors of the F1 and F2 adult offspring.[35] Importantly, the transgenerational effects manifested despite the behavior and daily sperm production of the treated F0 males remaining unaffected.[35,36] They were, however, accompanied by marked changes in the sperm sncRNA profile, with a focus for this study being the alteration of a subset of microRNAs (miRNAs) predicted to interact with multiple growth factors.[35] Consistent

with this response to sustained elevation of glucocorticoids, independent studies have also shown that as few as 10 days of restraint stress can affect changes in the sperm sncRNA landscape associated with downstream metabolic health disturbance in the F1 generation.[37–39] Similarly, models focusing on dietary toxicants have reported changes to sperm sncRNAs following as few as 5 days of exposure.[29] Such rapid responses to imposed stressors firmly implicates the epididymis as a potential site for relaying stress related sncRNA signals to spermatozoa.

A potential link between these responses to divergent stress models is the innervation of conserved stress response pathways.[29] In this context, our recent work traced the differential accumulation of toxicant-responsive sncRNAs to coincide with sperm transit of the proximal (caput) segment of the epididymis, wherein we detected elevated expression of several transcription factors in the lining epithelium, including that of the glucocorticoid receptor, NR3C1 (nuclear receptor subfamily 3, group C, member 1).[29] NR3C1 serves as a master regulator of other transcription factors and one that is capable of driving the expression of a spectrum of glucocorticoid responsive genes.[40] Despite these findings, comparatively little is known regarding the role of NR3C1 in normal epididymal function nor in directing the response of this tissue to paternal stress.[41–43] Accordingly, here we sought to model the stress response of the epididymis via the imposition of a corticosterone challenge on an immortalized caput epididymal cell line (mECap18).[44] Among the advantages of this approach is that it eliminates potential confounding effects attributed to stress-related neuroendocrine dysregulation of hypothalamic–pituitary–adrenal axis activity in an animal. Whilst acknowledging limitations associated with an inability to replicate the precise epididymal microenvironment and physiological blood perfusion under in vitro conditions, this tractable model has afforded novel insight into the complexity of the molecular signaling responses elicited in male reproductive tissues following direct corticosterone challenge.

2 | MATERIALS AND METHODS

2.1 | Chemicals and reagents

All reagents were purchased from Merck (Darmstadt, Germany), unless otherwise specified.

2.2 | Animals and ethics statement

All experimental procedures were conducted with the approval of the University of Newcastle's Animal Care and Ethics Committee (ACEC; approval number A-2017-726), in accordance with national and international guidelines. Swiss mice were obtained from the University of Newcastle's Central Animal House and were housed under a controlled lighting regimen (12 h light, 12 h dark) at 21—22°C and supplied with food and water ad libitum. Animals were acclimated for at least 1 week prior to treatment. Swiss mice (adult males of at least 8 weeks of age) were utilized for all experiments and were euthanized via CO_2 inhalation, prior to having their vasculature perfused with pre-warmed TBS to eliminate blood contamination. The epididymides and vas deferens were dissected and separated from fat and connective tissue. The epididymides were carefully divided into three anatomical segments, corresponding to the caput, corpus, and cauda epididymis and the segment of interest was prepared for isolation of epithelial cells as previously described.[45]

2.3 | mECap18 cell culture, corticosterone, and everolimus treatment

The SV40-immortalized mouse caput epididymal epithelial (mECap18) cell line was generated from the dissected epididymides of one cohort of 4- to 5-month-old mice as we have previously described.[44] Aliquots of 4×10^5 mECap18 cells were passaged in each well of six-well plates and cultured in Dulbecco's modified Eagle medium (DMEM) (4.5 g/L glucose) supplemented with 100 μM sodium pyruvate, 200 μM L-glutamate, 100 U/mL penicillin, 10 μg/mL streptomycin, and 10% (v/v) heat inactivated fetal bovine serum with 50 nM 5α-androstan-17β-ol3-one.[46] Cells were plated and allowed to grow for 48 h prior to treatment with either 100 nM 4-pregnen-11β, 21-diol-3, 20-dione 21-acetate (corticosterone; Steraloids Inc, RI, USA) or dimethyl sulfoxide (DMSO) vehicle control for up to 10 days, with media/treatment replacement occurring at intervals of 48 h.[47] Importantly, neither of the treatments used in this study compromised mECap18 cell viability, which consistently remained >90% across the entire incubation period. Cells were harvested on days 3, 5, 7, and 10 post-treatment by pelleting (400×*g*, 5 min) and washing three times in TBS prior to performing protein extraction for assessment of the abundance of the NR3C1 glucocorticoid receptor. Alternatively, cells harvested on day 10 post-treatment were prepared for proteomic and phosphoproteomic analysis as described below. For assessment of DNA damage sustained as a consequence of corticosterone treatment, mECap18 cells were grown as described above but with the inclusion of an additional treatment group supplemented with the allosteric mTOR inhibitor, everolimus.[48] Specifically, mECap18 cells were pre-treated with everolimus (1 nM) for 1 h prior to the addition of corticosterone at each media replacement.

2.4 | SDS-PAGE and immunoblotting

After washing, mECap18 cells and epididymal epithelial cells were re-suspended in SDS extraction buffer (0.375 M Tris pH 6.8, 2% (w/v) SDS, 10% (w/v) sucrose, protease inhibitor cocktail), incubated at 100°C for 5 min and equivalent amounts of protein (10 μg) were separated by SDS-PAGE.[49] Gels were transferred onto nitrocellulose membranes (Hybond C-extra; GE Healthcare, Buckinghamshire, UK).[50] Membranes were blocked for 1 h in TBS containing 5% (w/v) skim milk powder. After rinsing with TBS containing 0.1% (v/v) Tween-20 (TBST), membranes were sequentially incubated with appropriate primary

antibody at 4°C overnight and the corresponding HRP-conjugated secondary antibody for 1 h. Primary antibodies used were as follows: anti-NR3C1 antibody (1:1000; #HPA004248), anit-BRCA1 antibody (1:1000; #9025S; Cell Signaling), anti-BRCA1 Serine 1524 (1:1000; #9009S; Cell Signaling), anti-GAPDH (1:4000; #G9545), and alpha-tubulin (1:3000; #T5168). Following three washes in TBST, labelled proteins were detected using enhanced chemiluminescence reagents (GE Healthcare).

2.5 | Immunocytochemistry

mECap18 cells were fixed in 4% paraformaldehyde, washed three times with 0.05 M glycine in PBS and then applied to poly-L-lysine coated glass coverslips. The cells were permeabilized with 0.2% Triton X-100 and blocked in 3% bovine serum albumin (BSA)/PBS for 1 h. Coverslips were then washed in PBS and incubated in a humidified chamber with appropriate primary (anti-NR3C1 antibody; HPA004248; Merck) and secondary antibodies (1 h at 37°C). Coverslips were washed (3 × 5 min) in filtered PBS after each antibody incubation, before counterstaining with 4′,6-diamidino-2-phenylindole (DAPI) and mounting in antifade reagent comprising 10% Mowiol 4—88 (Merck), 30% glycerol, and 2.5% 1,4-diazobicyclo-(2.2.2)-octane in 0.2 M Tris (pH 8.5). After immunolabeling, mECap18 cells were examined by confocal microscopy (Olympus, Nagano, Japan) to determine target protein localization. A portion of mECap18 cells were also subjected to anti-γH2A.X (ab11174; Abcam, Cambridge, UK) labeling to assess levels of DNA damage sustained as a consequence of corticosterone treatment as previously described.[51] For this purpose, mECap18 cells were incubated with anti-γH2AX (diluted 1:500 with 1% BSA/PBST) before being washed and incubated with the appropriate fluorescent conjugated secondary antibodies (diluted 1:200 with 1% BSA/PBST) for 1 h at room temperature. Cells were counterstained with DAPI and images collected as described above before being imported to ImageJ for calculation of γH2A.X pixel intensity in at least 100 cells.

2.6 | RNA extraction and qPCR

mECap18 cells and epididymal epithelial cells were harvested from three biological replicates and RNA was isolated using a TRIzol RNA extraction method in accordance with the manufacturer's instructions. Briefly, spermatozoa were removed from epididymal tissue by placing the tissue in a 500 µL droplet of TBS and making multiple incisions with a razor blade. The tissue was then washed free of residual spermatozoa by subjecting it to agitation, prior to being minced with forceps and washed a further three times in TBS. Tissue was digested with 100 mg/mL trypsin (Promega, Madison, WI, USA) in TBS at 37°C for 30 min with vigorous shaking in a thermomixer. Clumped tissue sections were collected by centrifugation (800×*g* for 5 min) and then digested with 1.0 mg/mL collagenase type II in TBS for 30 min with shaking at 37°C. Cells were pelleted (800×*g* for 5 min) and resuspended in DMEM culture medium containing sodium pyruvate (1 mM), 10% (v/v) fetal bovine serum, 100 IU/mL penicillin, and 100 mg/mL streptomycin (Thermo Fisher Scientific, Waltham, MA, USA) prior to being filtered through a 70 µm membrane and incubated in six-well plates at 32°C for 4 h. This incubation facilitated the adherence of all non-epithelial cells to the bottom of the plate and their separation away from the epithelial cells, which remained in the suspension. Enrichment of epithelial cell populations was assessed by immunocytochemistry using the DAPI nuclear stain to identify contaminating spermatozoa.[45,51] For gene expression analysis, total cellular RNA (3.0 µg) was reverse transcribed using 500 ng Oligo(dT)15 primer, 5× buffer, 100 mM dithiothreitol, 40 Units (U) RNasin ribonuclease, 0.5 mM dNTPs, and 20 U of Moloney murine leukemia virus reverse transcriptase (all purchased from Promega). qPCR analysis was performed using primers targeting *Nr3c1*: forward (5′-GAGGACAACCTGACTTCCTTGGG-3′) and reverse (5′-GTGGTCCCGTTGCTGTGGA-3′) and the reference gene, *cyclophilin* [forward (5′- CGTCTCCTTCGAGCTGTTT-3′), reverse (5′-ACCCTGGCACATGAATCCT-3′)]. qPCR reactions were performed using a LightCycler 96 Instrument (Roche Life Science, Basel, Switzerland) at 95°C for 2 min, then 40 cycles of 95°C for 15 s and 56°C (*cyclophilin*) or 62°C (*Nr3c1*) for 1 min. The $2^{-\Delta Ct}$ method[52] was used to calculate *Nr3c1* abundance normalized to the *cyclophilin* reference.

For assessment of miRNA expression in mECap18 cells, TaqMan assays (Thermo Fisher Scientific), targeting *mmu-miR-20a-5p* (assay ID, 000580), *mmu-miR-30a-5p* (assay ID, 000417), *mmu-miR-152-3p* (assay ID, 000475), and *U6snRNA* (assay ID, 001973) were reverse transcribed from 10 ng RNA using TaqMan miRNA Reverse Transcription Kits (Thermo Fisher Scientific).[53] miRNA (0.7 ng) was amplified using 1× TaqMan Universal PCR master mix II, no UNG (Thermo Fisher Scientific), and 1× TaqMan miRNA PCR primer probes in a LightCycler 96 Instrument (Roche) at 50°C for 2 min, 95°C for 10 min, then 40 cycles of 95°C for 15 s and 60°C for 1 min. The 2−ΔCt method[52] was used to calculate miRNA abundance normalized to *U6snRNA* reference.

2.7 | Proteomic sample preparation

mECap18 cells were prepared for proteome and phosphoproteomic analysis using EasyPhos methodology.[18,54,55] In brief, 250 µL of chilled lysis buffer (4% [w/v] sodium deoxycholate; 100 mM Tris–HCl [pH 8.5]) was added to each sample and immediately heated (95°C, 5 min) to inactivate endogenous proteases and phosphatases. Samples were sonicated (3 × 10 s cycles, 100% power output), and an aliquot taken for determination of protein concentration using a bicinchoninic acid assay. All samples were diluted to equal protein concentration in lysis buffer (90 µg/270 µL) in 2 mL deep well plates. The samples were then mixed (1:10, v/v) with a stock solution of reduction/alkylation buffer comprising 100 mM TCEP and 400 mM 2-chloroacetemide (i.e., final working concentration 10 mM TCEP and 40 mM 2-chloroacetemide) using a Thermoshaker. For this purpose, samples were incubated for 5 min at 45°C with shaking at 1500 rpm. Enzymatic digestion was achieved using a trypsin/Lys-C mixture, at an enzyme-to-substrate ratio of 1:30 (w/w), and incubated overnight at 37°C with shaking at

1500 rpm. Phosphopeptides were enriched using titanium dioxide and, in parallel with their corresponding proteome peptides, desalted using styrenedivinylbenzene-reverse phase sulfonated StageTips[56] prior to analysis using high resolution nano liquid chromatography tandem MS (nLC–MS/MS).

2.8 | nLC–MS/MS analysis

Reverse phase nLC–MS/MS was performed using an Orbitrap Exploris 480 MS coupled to a Dionex Ultimate 3000RSLC nanoflow high-performance liquid chromatography system (Thermo Fisher Scientific). Samples were loaded onto an Acclaim PepMap 100 C18 75 μm × 20 mm trap column (Thermo Fisher Scientific) for pre-concentration and online de-salting. Separation was then achieved using an EASY-Spray PepMap C18 75 μm × 250 mm column (Thermo Fisher Scientific), employing a linear gradient of acetonitrile (2–35%, 130 min; 35–95%, 4 min) over 160 min for non-modified peptides, and a linear gradient of acetonitrile (2–35%, 90 min; 35–95%, 4 min) over 120 min for phosphorylated peptides. Full MS/data-dependent acquisition MS/MS mode was utilized on Xcalibur (Thermo Fisher Scientific; version 4.2.47) with the Orbitrap mass analyzer set at a resolution of 60,000, to acquire full MS with an *m/z* range of 350–1500, incorporating a normalized automatic gain control target of 300% and maximum fill times of 100 ms. The 20 most intense multiply charged precursors were selected for higher-energy collision dissociation fragmentation with a collisional energy of 30. MS/MS fragments were measured at an Orbitrap resolution of 15,000 using standard mode for automatic gain control target and maximum fill time mode set to auto.

2.9 | Data processing and analysis

In accordance with previous studies,[26,55,57–61] database searching was performed for the mECap18 proteome and phosphoproteome using Proteome Discoverer 2.5 (Thermo Fisher Scientific). SEQUEST HT was used to search against the UniProt *Mus musculus* database (63,717 sequences, downloaded February 25, 2021). Database searching parameters included up to two missed cleavages, a precursor mass tolerance set to 10 ppm, fragment mass tolerance of 0.02 Da, and trypsin designated as the digestion enzyme. Cysteine carbamidomethylation was set as a fixed modification while dynamic modifications included acetylation (N-terminus), oxidation (M), and phosphorylation (S/T and Y). PhosphoRS[62] was employed for accurate site-specific assignment of phosphorylation, with a threshold minimum cut-off 75% assignment to final refined of sites. Interrogation of the corresponding reversed database was also performed to evaluate the false discovery rate (FDR) of peptide identification using Percolator based on q-values, which were estimated from the target-decoy search approach. To filter out target peptide spectrum matches over the decoy-peptide spectrum matches, a fixed FDR of 1% was set at the peptide level. Mass recalibration and label-free quantification (LFQ) of area under the curve MS1 peaks were conducted using Proteome Discoverer nodes, Spectrum Files RC, Minora Feature Detector, and Feature Mapper.[61] Fold changes in phosphopeptide/protein abundance and statistical significance between control and corticosterone-treated groups were calculated by Proteome Discoverer 2.5 using a non-nested pairwise ratio approach. The protein list was exported as an Excel file and further refined to include only those proteins with a quantitative value (e.g., raw, normalized and scaled values) in at least three replicates within at least one group and a minimum of two unique peptides. Further to this, proteins with one unique peptide were included if the coverage sequence (%) of that protein was equal to, or greater than, the average sequence coverage of the full complement of proteins with two or more unique peptides (30% coverage). Using Perseus (version 1.6.10.43),[63] Pearson correlation plots and principal component analyses were generated from normalized and scaled data, respectively, and graphed using GraphPad Prism version 9.1.1 for Windows (GraphPad Software, San Diego, CA, USA).

2.10 | Ingenuity pathway analysis

Ingenuity pathway analysis (IPA) software (Qiagen, Hilden, Germany) was used to analyze refined proteomic and phosphoproteomic lists as previously described.[55,57,60,61,64–66] Briefly, canonical pathways, upstream regulators, and disease and function analyses generated using IPA were assessed using: (i) *p* values—an enrichment measurement of the overlapping proteins from the dataset in a particular pathway, function or regulator, and (ii) *Z*-score—a prediction scoring algorithm of activation or inhibition based upon statistically significant patterns in the dataset and prior biological knowledge manually curated in the Ingenuity Knowledge Base.[67] To elucidate the most significant changes in our analyses, we applied a stringency criteria *p*-value of ≤ 0.05 and a *Z*-score of (inhibition) $-2 \leq Z \geq 2$ (activated).

2.11 | miRNA target prediction

The online database miRDB (http://mirdb.org/)[68,69] was utilized to obtain a list of predicted miRNAs targets to identify their potential function. Each of the three miRNAs investigated (*miR-20a-5p*, *miR-152-3p*, and *miR30a-5p*) were submitted to miRDB under *M. musculus*, and the resulting targets were refined to those that had a prediction score of at least 80 out of 100, as per miRDB instructions, prior to submission to IPA for further analysis.

2.12 | Kinase-substrate PhosphoSitePlus analysis

The Kinase-substrate dataset of PhosphoSitePlus (http://www.phosphosite.org/, an open-source curated resource for investigating the importance of experimentally observed post-translational modifications in the regulation of biological processes,[70] was downloaded (accessed May 5, 2021) to identify kinases implicated in the phosphorylation of the specific amino acid motifs identified in significantly

altered phosphopeptides. Please see Supplementary File 1 for a detailed step-by-step guide for how this was achieved. In brief, first the downloaded kinase-substrate dataset was opened using Excel (for descriptive purposes this will be called Excel F1) and separated out into individual columns using the *text to column* function. This provides all annotated sites ±7 amino acids (column L) to known upstream kinases (column R). Next, the full *M. musculus* proteome (10090 proteins) was downloaded from UniProt as an excel sheet (Excel F2) including columns for *Entry*, *Entry Name*, *Protein Name*, *Gene Name* and *Sequence*, compatible with mapping the identified phosphopeptides. Using the formulas detailed in Supplementary File 1, a second sheet within Excel F2 generates a table whereby the user enters the sequence of the phosphopeptide of interest, its corresponding UniProt Accession and the phosphorylated residue, and the table will orientate the phosphorylated residue of interest to the center of an annotated sequence within the surrounding amino acids (±7) in the parent protein (e.g., ATP7A site S1454; ivnysraSinsllsd). With the sequences in the format compatible to the PhosphoSite database, the phosphopeptide of interest will be mapped to its upstream kinase(s) if a known relationship exists.

2.13 | Experimental design and statistical rationale

Phosphoproteomic analyses were performed using mECap18 ($n = 4$ biological replicates collected from four unique cell cultures derived from the original mECap18 cell line). Differentially abundant proteins/phosphopeptides were defined as those with a fold-change ≥1.5 or ≤−1.5 and p value ≤0.05. All other data were assessed for normality using the Shapiro-Wilk normality test. Normally distributed data were analyzed by unpaired Student's t-tests to detect differences between treatment groups. Data not normally distributed were analyzed by a Mann–Whitney U test. Differences between groups were considered significant when $p \leq 0.05$. A one-way ANOVA statistical test, with Tukey multiple correction, was applied to transcriptomic, real time, and immunoblotting quantification of NR3C1 from caput, corpus, cauda epididymal tissue and from mECap18 cells. The number of biological replicates used in each experiment is presented in the figure captions. Graphical data were prepared using GraphPad Prism version 9.1.1 for Windows (GraphPad Software) and are presented as mean values ± SEM.

3 | RESULTS

3.1 | The NR3C1 glucocorticoid receptor is abundantly expressed in caput epididymal epithelium

As a prelude to studying the molecular adaptation of the epididymal epithelium to acute corticosterone challenge, we first examined the intraepididymal expression profile of the glucocorticoid receptor [nuclear receptor subfamily 3 group c member 1 (NR3C1)], whose presence is a prerequisite for manifestation of cellular responses to this stress hormone. For this analysis, we initially accessed curated *Nr3c1* transcript expression data from an independent microarray study of gene expression in the mouse epididymis.[71] As is common practice, expression data were summed across those regions comprising the caput (segments 2—5), corpus (segments 6—7), and cauda (segments 8—10) epididymis, revealing the highest levels of *Nr3c1* expression in the caput, followed by that of the cauda and corpus epididymal segments (Figure 1A). These data were orthogonally validated in three biological replicates via RT-qPCR amplification of the *Nr3c1* transcript (Figure 1B) and by immunoblotting of epididymal tissue homogenates with anti-NR3C1 antibodies (Figure 1C and Supplementary File 2), both of which confirmed equivalent trends of *Nr3c1* gene expression and NR3C1 protein abundance to those identified by microarray analysis. Together, these in vivo *Nr3c1* expression data informed our subsequent focus on the caput epididymis as the segment most likely to be sensitive to stress-elicited surges in circulating corticosterone concentrations. Moreover, they also justified our use of an immortalized mouse caput epididymal epithelial cell line (mECap18)[44,72,73] as a tractable tool for modeling the response of the epididymis to direct corticosterone challenge independent of potentially confounding effects associated with whole body exposure paradigms.

Accordingly, we confirmed endogenous *Nr3c1* gene expression and protein abundance in naive mECap18 cells at levels that were comparable to that of caput epididymal tissue (Figures 1B and C and Supplementary File 2). Despite this, the NR3C1 protein abundance levels in mECap18 cells treated with corticosterone over a time course of 10 days failed to track with those previously documented for *Nr3c1* gene expression under an identical exposure regimen.[47] Thus, although previous studies have shown a marked increase in mECap18 *Nr3c1* gene expression between 7- and 10-days post-corticosterone exposure,[47] here there was no statistically significant increase in NR3C1 protein abundance at either of these time points (Figures 1D and E and Supplementary File 2). Immunocytochemistry staining of mECap18 cells at day 10 post-treatment confirmed no significant difference in the level of NR3C1 protein expression or cellular localization (Figure 1E). Such findings do not, however, preclude an upregulation of steroid-binding capabilities and/or functional activation of the NR3C1 glucocorticoid receptor leading to the initiation of downstream signaling pathways that direct the stress response of the host cell. To explore this possibility, mECap18 cells were challenged with corticosterone for 10 days prior to being prepared for analysis of changes in their global proteomic profile as well as that of the phosphoproteomic signature.

3.2 | The core mECap18 cell proteome is subtly altered by corticosterone challenge

Corticosterone challenged mECap18 cells were subjected to high-resolution phosphoproteomic analysis using an EasyPhos protocol[54] to enable simultaneous analyses of the cell proteome and the respective site-specific phosphorylation events. This experimental strategy

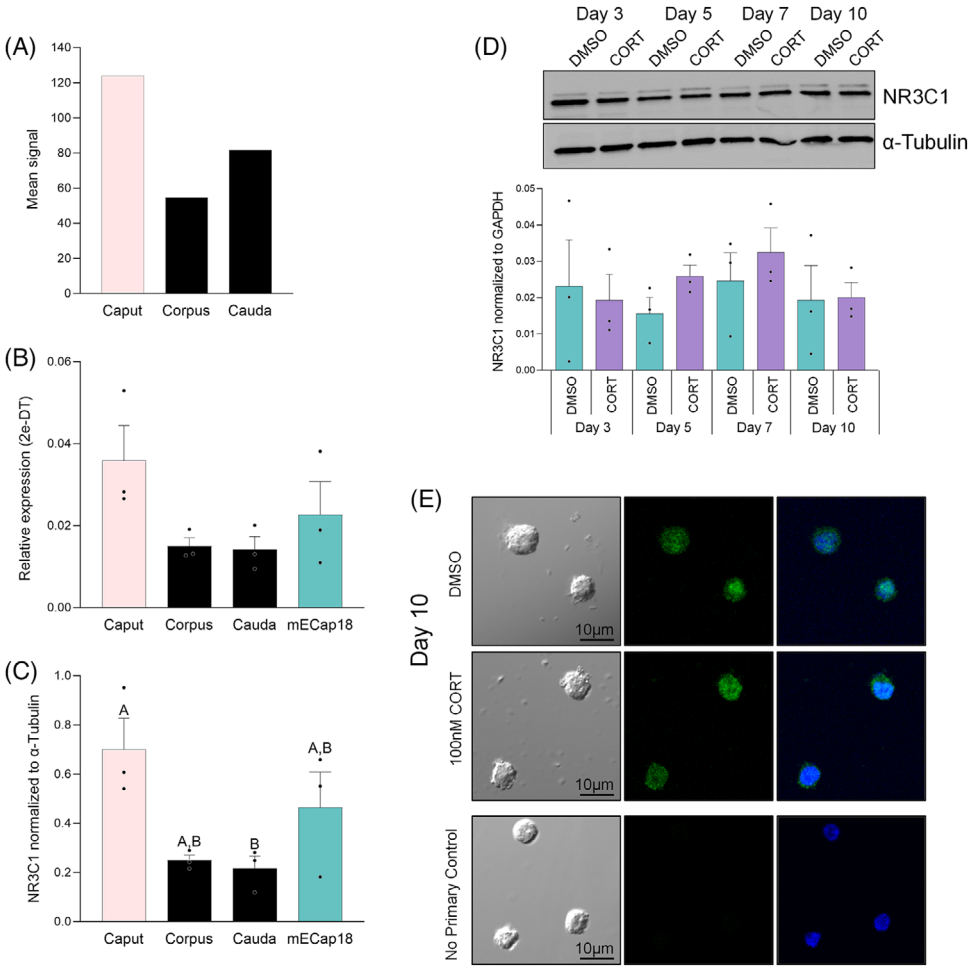

FIGURE 1 cGlucocorticoid receptor (NR3C1) transcript and protein levels in mouse epididymal epithelial cells. (A) Transcriptomic expression of the glucocorticoid receptor (*Nr3c1*) in caput, corpus, and cauda epididymal segments as reported in the publicly available Mammalian Reproductive Genetics database (http://mrgd.org/; accessed 1/8/2021). (B) Real time expression confirmed the presence of *Nr3c1* in caput, corpus, cauda epididymal tissue, and the immortalized mouse caput epididymal (mECap18) cell line ($n = 3$). (C) Immunoblotting densitometry quantification of NR3C1 protein levels in caput, corpus, cauda epididymal tissue, and mECap18 cells relative to the alpha-tubulin loading control ($n = 3$). A connecting letter plot is depicted to denote which segments featured significantly different NR3C1 abundance ($p \leq 0.05$). (D) Time course treatment of mECap18 cells with DMSO (green columns) or corticosterone (CORT; purple columns), with protein quantification of NR3C1 relative to the alpha-tubulin loading control, following 3, 5, 7, and 10 days post-treatment ($n = 3$). (E) Representative images of mECap18 cells labeled with anti-NR3C1 antibodies (green) and counterstained with DAPI (blue) after 10 days of treatment with either DMSO vehicle or CORT, including minus primary antibody control. A one-way ANOVA statistical test, with Tukey multiple correction used, was applied to panels A–C. Mean ± SEM, with individual datapoints, are plotted in bar charts. All *n* sizes refer to number of biological replicates.

identified a complex proteomic signature comprising a total of 4159 and 4161 proteins in vehicle and corticosterone-treated cells, respectively. As demonstrated, Pearson's correlation coefficient values of between 0.981 and 0.993 (based on normalized data) confirmed a strong positive relationship between each of the four biological replicates featured in this quantitative analysis (Figure 2A). Moreover, an average of 10.5 peptide matches were generated per protein (encompassing ≥9.3 unique peptide mapped/protein), representing an average peptide coverage of 29.5% per protein; data that attest to both the stringency of the criteria imposed for positive protein identification and the depth of coverage achieved in this proteomic dataset (Figure 2B and Table S1). In comparing the core proteome of vehicle control and corticosterone-treated mECap18 cells, we noted a substantial overlap of 99.5% of all identified proteins, with only 10 out of 4171 proteins being uniquely identified in vehicle control cells and a further 12 proteins being restricted to the corticosterone-treated population (Figure 2C). Despite this high level of overall protein conservation, a principal component analysis based on the relative abundance of these shared proteins, clearly differentiated the proteomic signature of the two cell populations and also demonstrated clustering of their biological replicates (Figure 2D). Provisional interrogation of the core mECap18 cell proteome based on cellular location revealed that among the 4103 proteins able to be mapped by IPA, the majority were localized to the cytoplasm (53.8%), followed by the nucleus (30.2%), plasma membrane (8.4%), and extracellular space (3.2%) (Figure 2E). Protein function classification returned the top

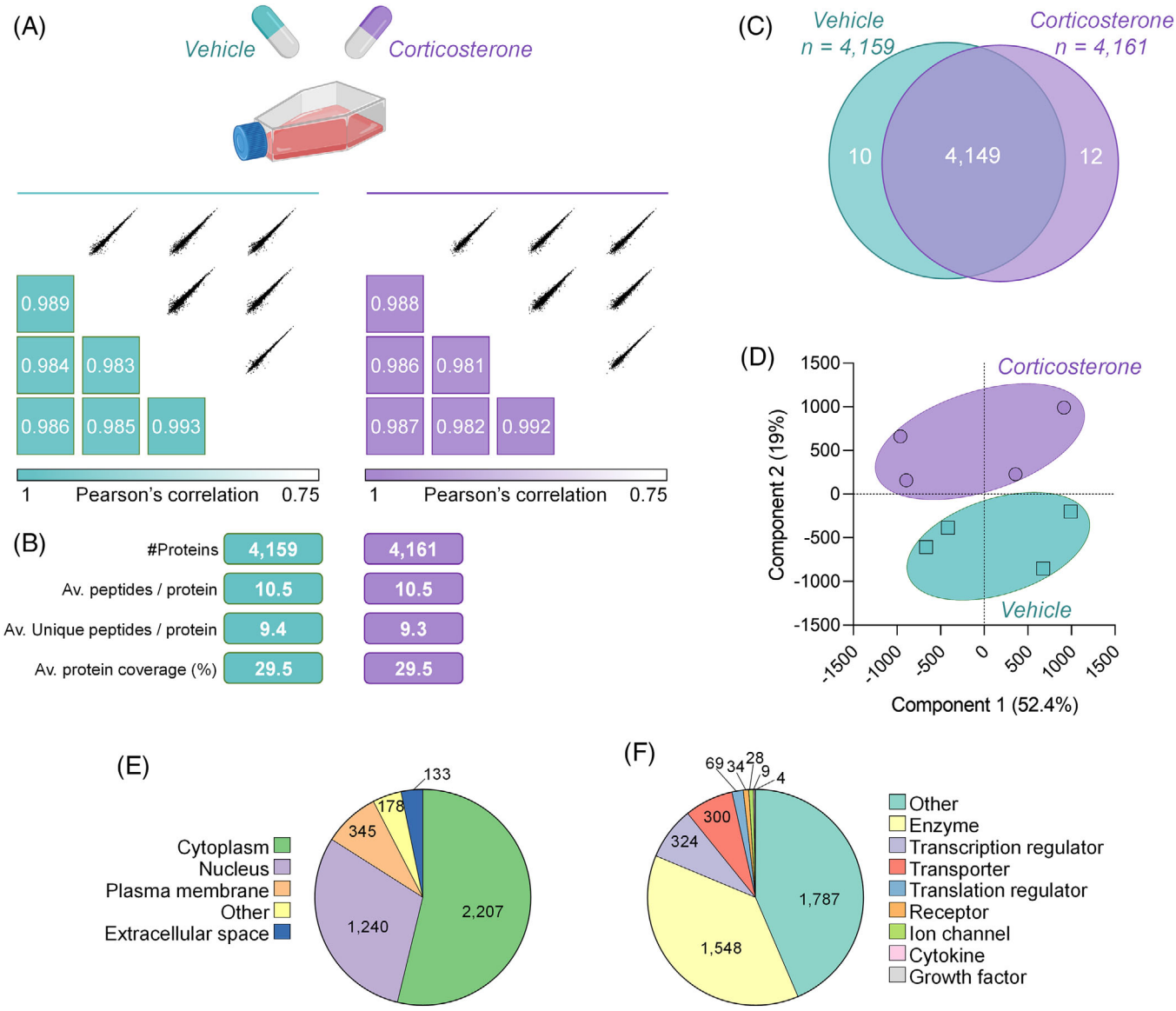

FIGURE 2 Proteomic characterization of mECap18 cells exposed to corticosterone. (A) Pearson correlation plots of four biological replicates for treatment with either vehicle (green) or corticosterone (purple). (B) Proteomic coverage depth for each treatment (vehicle—4159; corticosterone—4161) with their respective average number of peptides per protein, unique peptides per protein and average coverage sequence of proteins identified. (C) Venn diagram depicting the unique number of proteins to each treatment and the shared identities. (D) Principal component analysis (PCA) of each treated cell population; vehicle (green squares) or corticosterone (purple circles). (E) Assessment with Ingenuity Pathway Analysis of cellular localization and (F) protein classification.

five dominant categories of enzyme (37.7%), transcription regulator (7.9%), transporter (7.3%), translation regulator (1.7%), and receptor (0.8%) when ranked on the basis of number of annotated proteins (Figure 2F).

In addition to the subset of proteins uniquely present in each sub-population of mECap18 cells (Figure 3A), we also noted a modest number of proteins whose relative abundance profiles were significantly altered in response to corticosterone challenge (Figure 3B). Thus, a total of 10 proteins were identified as being significantly down-regulated in corticosterone-treated mECap18 cells, whilst a further 41 were upregulated under these experimental conditions (FC = ± 1.5, p value ≤ 0.05) (Figure 3B). IPA functional analysis of the combined inventory of mECap18 proteins either uniquely detected (Figure 3A; i.e., 22 proteins) or whose abundance was significantly altered in response to corticosterone challenge (Figure 3B; i.e., 51 proteins) predicted the activation of stress response regulators, such as nuclear factor-erythroid factor 2-related factor 2 (NRF2), cellular tumor antigen p53 (TP53), and RAC-alpha serine/threonine-protein kinase (AKT1) (Figure 3C and Table S2). Additionally, IPA predicted the activation of pathways associated with stress-activated protein kinases (SAPK)/Jun amino-terminal kinases (JNK) signaling (SAPK/JNK), paxillin signaling and NRF2-mediated oxidative stress response. By contrast, IPA predicted the inhibition of POU domain, class 5, transcription factor 1 (POU5F1), tumor necrosis factor receptor

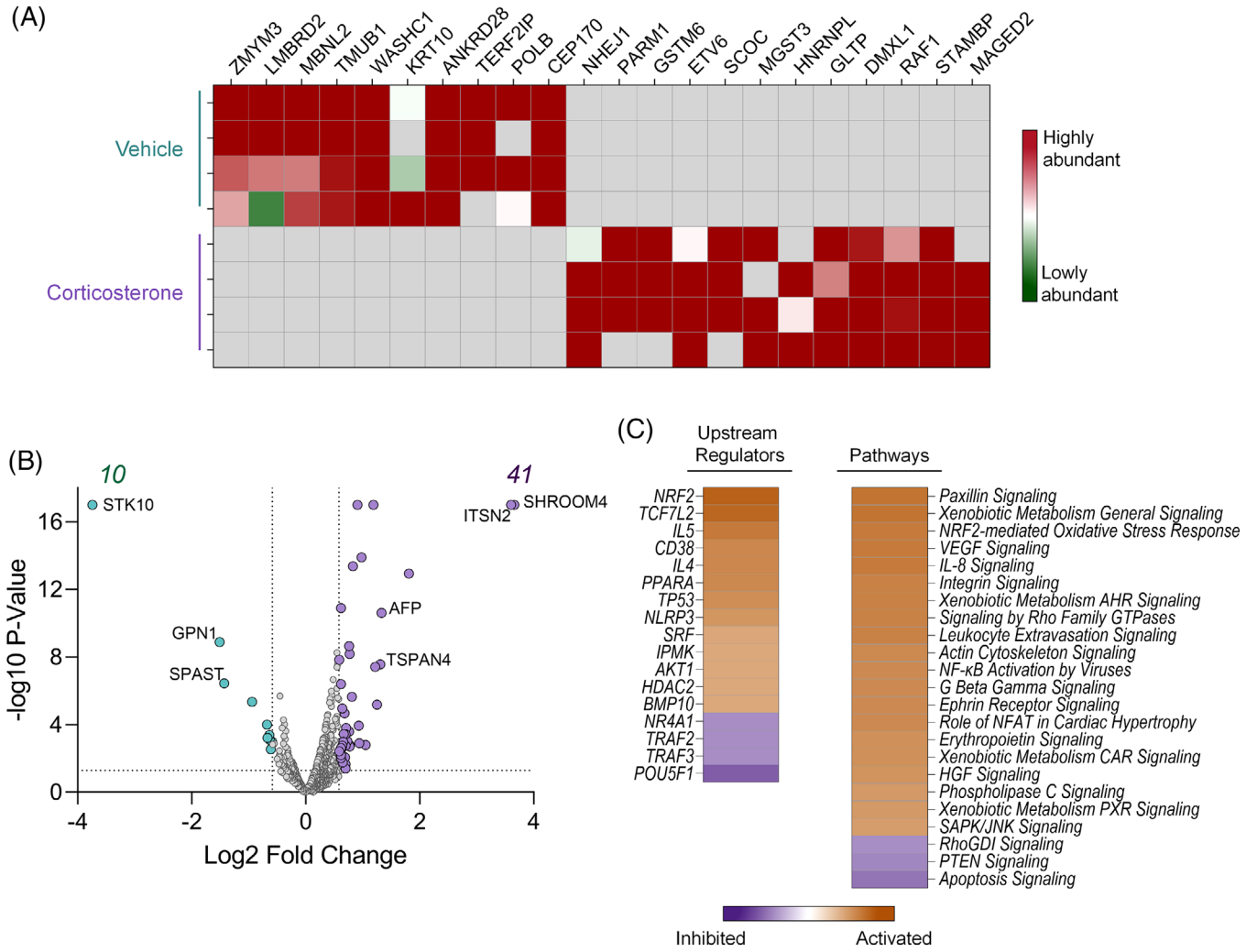

FIGURE 3 Quantitative analyses of mECap18 protein abundance following corticosterone treatment. (A) Heat map depicting the unique proteins detected in both treatment groups, with abundance levels. (B) Volcano plot analysis revealed 41 upregulated proteins and 10 downregulated proteins following corticosterone treatment; $\log_2$ fold change (*x*-axis) and −log *p* value (*y*-axis) with thresholds of ±1.5 fold change and *p* value of ≤0.05. (C) Ingenuity Pathway Analysis of the predicted activated and inhibited upstream regulators and pathways.

associated factor 2 (TRAF2), and 3 (TRAF3), as well as signaling pathways associated with apoptosis, PTEN, and RhoGDI (Figure 3C and Table S2).

3.3 | Corticosterone challenge is linked to DNA damage repair and RNA biogenesis signaling pathways in mECap18 cells

To expand our analysis of the cellular response mounted to corticosterone challenge, phosphopeptide-enrichment was performed in tandem with LFQ to identify signatures of stress-associated signaling within mECap18 cells. Complementing the depth of global proteomic coverage achieved, a complex phosphoproteomic inventory comprising 5345 and 5330 phosphopeptides (average 94% phospho-enrichment) was identified in vehicle and corticosterone-treated mECap18 cells, respectively (Table S3). Pearson's correlation coefficient values of between 0.933 and 0.977 confirmed a strong positive relationship between each of the four biological replicates featured in this analysis (Figure 4A). The mapping of these phosphopeptides to 1916 and 1911 unique proteins in vehicle and corticosterone-treated cells (Figure 4B), respectively, revealed that a substantial portion of the mECap18 proteome harbored multiple phosphopeptides (i.e., an average of 2.8 phosphorylated peptides identified per protein). More specifically, 871 proteins were identified with a single phosphopeptide versus 1045 proteins that possessed ≥2 phosphopeptides (Figure 4C). Among these phosphorylation events, serine residues were the most abundant target, accounting for ~77% of all differentially phosphorylated sites (Figure 4D). Thereafter, threonine was the next most common phospho-target (~5%), with only relatively few tyrosine residues (~0.2%) being identified as differentially phosphorylated in our analysis (Figure 4D). Amongst the phosphorylated peptides identified, 362 (6.7%) were found to have a non-phosphorylated counterpart (Table S3).

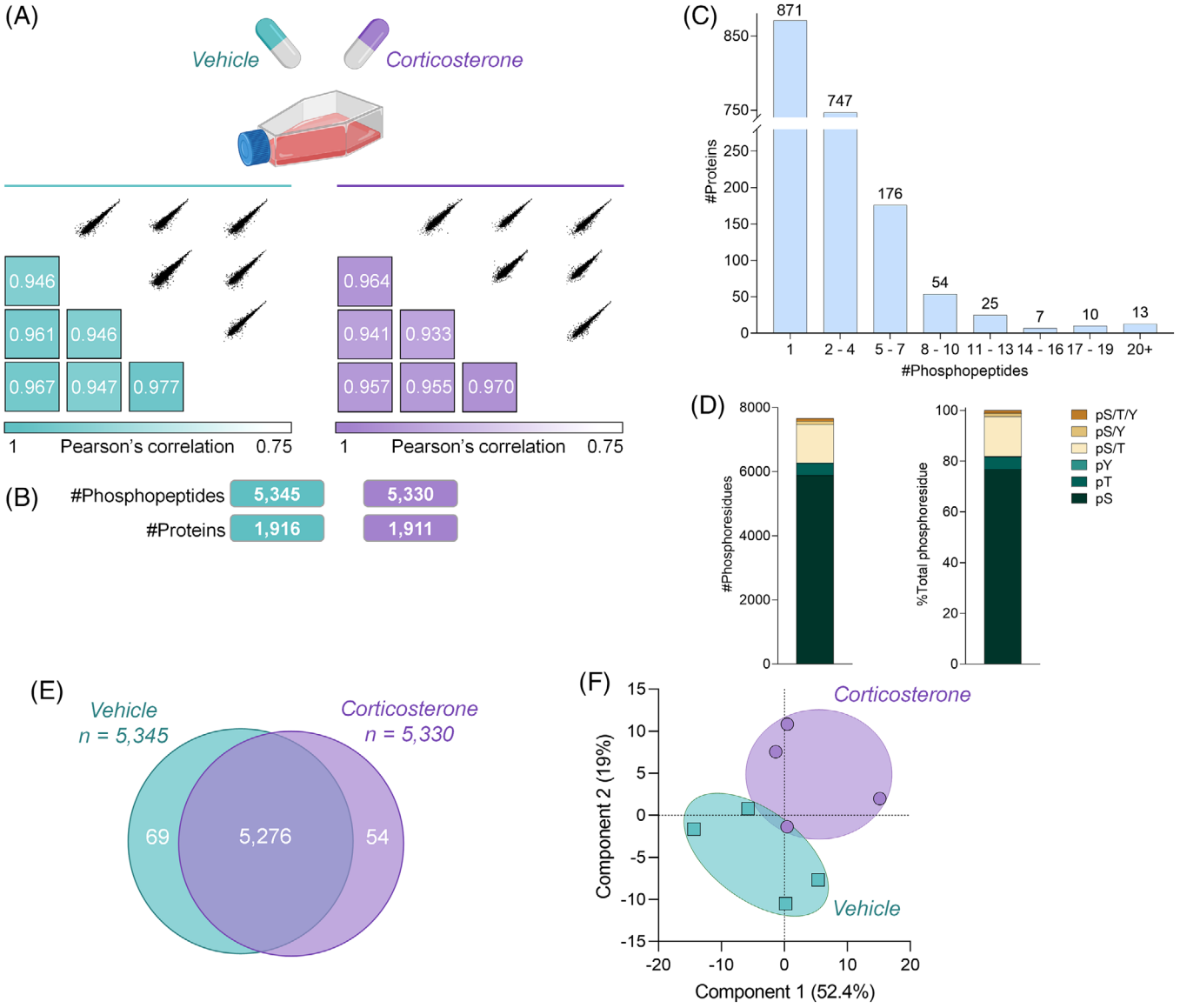

FIGURE 4 Phosphoproteomic assessment of mECap18 cells exposed to corticosterone. (A) Pearson correlation plots of four biological replicates for treatment with either vehicle (green) or corticosterone (purple). (B) Number of unique phosphopeptides for each treatment and parent proteins. (C) The distribution of how many proteins (*y*-axis) account for the identified phosphopeptides (*x*-axis). (D) The total number and proportional distribution of phospho-serine (pS), -threonine (pT), and -tyrosine residues (pY) for all phosphopeptides; pS/T, pS/Y, pS/T/Y = ambiguous phosphorylation of either: a serine or threonine residue, a serine or tyrosine residue, or a serine, threonine, or tyrosine residue, respectively. (E) Venn diagram depicting the unique number of proteins to each treatment and the shared identities. (F) Principal component analysis (PCA) of each treated cell population; vehicle (green squares) or corticosterone (purple circles).

Comparing the phosphoproteomic signature of vehicle control and corticosterone-treated mECap18 cells, an overlap of 97.7% was detected among all identified phosphopeptides, with only 69 out of 5394 phosphopeptides being exclusively identified in vehicle control cells and an additional 54 phosphopeptides being restricted to the corticosterone-treated population (Figure 4E). In accordance with this high level of conservation, principal component analyses did not definitively separate the two cell populations on the basis of their phosphopeptide signature (Figure 4F). In expanding this analysis to consider those phosphopeptides that experienced a threshold of ±1.5 fold-change, we identified a further 362 out of 5394 (~6.7%; Figure 5A) phosphopeptides that were differentially phosphorylated in vehicle versus corticosterone-treated mECap18 cells. Among these phosphopeptides, 150 were significantly under-represented and a further 212 were significantly over-represented in the latter population of corticosterone-treated mECap18 cells. Within this restricted subset of phosphopeptides, 190 harbored multiple phosphorylation sites and several additional candidates mapped to proteins possessing multiple phosphopeptides. Thus, 49 proteins were identified as being targeted for multiple (de)phosphorylation events, with prominent examples including: serine/arginine repetitive matrix protein 2 (SRRM2), A-kinase anchor protein 12 (AKAP12), tensin 1 (TNS1), and nuclear

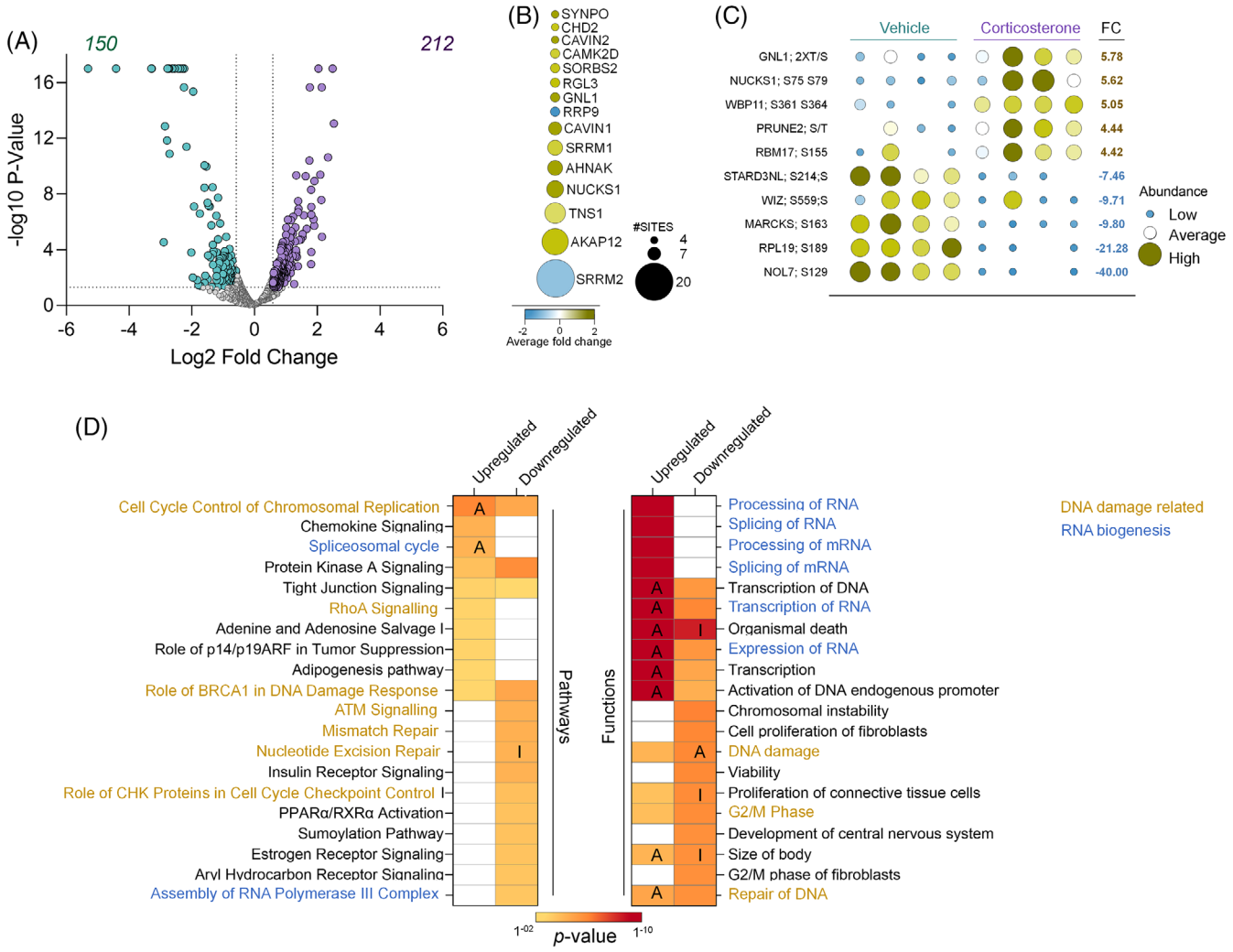

FIGURE 5 Functional analyses of adaptive phosphoproteome response of mECap18 cells exposed to corticosterone. (A) Volcano plot analysis revealed 362 unique phosphopeptides are significantly dysregulated due to corticosterone; $\log_2$ fold change (*x*-axis) and −log *p* value (*y*-axis) with thresholds of ±1.5 fold change and *p* value of ≤0.05. (B) Top 15 multi-phosphorylated parent proteins; size of circle proportional to number of phosphorylated sites and color denoted fold change. (C) The five peptides with largest fold changes observed for both increase and decreased levels of phosphorylation; size and color of circle proportional to abundance of biological replicate. (D) Comparative functional analysis of the parent proteins that experienced significantly increased or decreased phosphorylation in response to corticosterone treatment. Heatmaps represent the top 10 significant (*p* value) pathways and downstream functions from ingenuity pathway analysis. A, predicted activation; I,= predicted inhibition. Pathways and downstream functions related to DNA damage and repair, or RNA biogenesis are highlight in gold and blue, respectively.

ubiquitous casein and cyclin-dependent kinase substrate 1 (NUCKS1), each with as many as 20, 14, 11, and 9 differentially phosphorylated residues, respectively (Figure 5B and Table S3). Together, the combination of exclusively identified (123) and significantly altered phosphopeptides (362) were mapped to a total of 350 unique parent proteins. Moreover, taking into account the multiple (de)phosphorylation events that occurred across these peptides/proteins, we identified 813 site specific phosphorylation events as being altered between vehicle and corticosterone-treated mECap18 cells, representing a substantial 15.1% of all phosphosites detected in this study (Table S4).

Overall, among the altered and unique phosphopeptides, proportionally more experienced increased, as opposed to reduced, phosphorylation in corticosterone-treated mECap18 cells versus that of their vehicle-treated counterparts (i.e., 266 vs. 219, respectively; Tables S3 and S4). The former of these corticosterone-associated changes included several phosphopeptides that more than doubled their basal levels documented in vehicle control-treated mECap18 cells (Figure 5C and Tables S3 and S4). Among the most dominant of these were peptides mapping to associated/modulators of pro- and anti-apoptotic proteins such as guanine nucleotide-binding protein-like 1 (GNL1), NUCKS1 and protein prune homolog 2 (PRUNE2), as well as regulators of RNA splicing, WW domain-binding protein 11 (WBP11) and splicing factor 45 (RBM17) (Figure 5C). Alternatively, phosphopeptides mapping to proteins such as nucleolar protein 7 (NOL7), 60S ribosomal protein L19 (RPL19), and myristoylated alanine-rich C-kinase substrate (MARCKS) were characterized by a substantial reduction in

their abundance in corticosterone-treated mECap18 cells (Figure 5C and Tables S3 and S4).

Pathway analysis of the parent proteins that experienced significantly increased phosphorylation, or were uniquely phosphorylated, in response to corticosterone treatment identified several pathways related to DNA damage and its response elements, including cell cycle control of chromosomal replication, RhoA signaling, and BRCA1 in DNA damage response (DDR) (Figure 5D and Table S5). Notably, the opposing subset of mECap18 cell proteins characterized by either a significant reduction in phosphorylation or complete dephosphorylation following corticosterone exposure, mapped to pathways related to DNA damage, identifying ataxia telangiectasia mutated (ATM) signaling (a known interactor of BRCA1 in DDRs),[74] mismatch repair signaling, and predicted inhibition of nucleotide excision repair. Analysis of downstream functions in IPA yielded overlap between proteins whose phosphorylation status was increased or reduced upon corticosterone treatment, both mapping to broadly similar functional categories. However, a clear distinction was the predicted activation of DNA damage. Amongst the many shared functions, both subsets of proteins exhibited reciprocal trends for activation/inhibition of repair of DNA and organismal death, suggesting that regulation of mECap18 cellular response is tightly coupled to the opposing action of cellular kinases and phosphatases (Figure 5D and Table S5). Moreover, comparison of this complex phosphoproteomic signature with curated DDR proteins,[75] identified 74 DDR proteins (258 phosphopeptides; Table S3). Another notable category identified by these analyses was RNA biogenesis (Figure 5D). Activation of the spliceosomal cycle was a predicted consequence of those proteins that experienced significantly increased phosphorylation, in addition to the predicted downstream activation of expression and transcription of RNA, as well as the unique identification of processing and splicing of RNA (Figure 5D and Table S5).

To assess if these stress-related signaling pathways identified in corticosterone-treated mECap18 cells are linked to downstream alterations in male reproductive tract biochemistry, we determined the relative abundance of three miRNAs, previously reported to be significantly reduced in caput epididymal cells from mice subjected to an in vivo stress model that also modulates *Nr3c1* expression.[51] In agreement with these previous observations, mECap18 cells subjected to corticosterone challenge featured a significant reduction in the abundance of *miR-20a-5p* and *miR-152-3p* ($p < 0.05$; Figures 6A and B). Whilst the detected change in *miR-30a-5p* expression did not achieve statistical significance, it did nonetheless trend towards an expected decrease (Figure 6C; p value = 0.087). Such findings are notable as the abundance of *miR-30a-5p* has previously been shown to be significantly altered in the mature spermatozoa of mice subjected to exogenous corticosterone treatment and thereafter linked to elevated anxiety and depression-related behaviors in the F1 and F2 adult offspring of corticosterone exposed sires.[35] To explore if this subset of miRNAs have the capacity to exert influence over downstream embryonic gene network pathways that could account for such a phenotype, each miRNA was submitted to the online database miRDB (http://mirdb.org/)[68,69] to curate predicted/known targets (prediction score ≥80). Subsequent IPA interrogation of each list of putative miRNA targets revealed a potential impact on several physiological system development networks and functions (Figures 6D and E). Chief amongst these networks were nervous system development and embryonic development (Figure 6D).

3.4 | DNA damage in corticosterone challenged mECap18 cells may be regulated via mTOR kinase activity

Interrogation of the PhosphoSitePlus database identified six kinases, each with confirmed expression in mECap18 cells and with known capability to drive the phosphorylation of at least four of the significantly regulated phosphorylated peptides (Table S6). Chief amongst the mapped kinases were casein kinase II subunit alpha (CK2A1), cyclin-dependent kinase 2 (CDK2) and cAMP-dependent protein kinase catalytic subunit alpha (PKACA) (Figure 7).

In agreement with the downstream pathway analyses (Figure 5D), five out of the six mapped kinases (CK2A1, CDK2, mechanistic target of rapamycin [mTOR], RAC-alpha serine/threonine-protein kinase [AKT1], and p38A; Figure 7) have been documented to possess key roles in DDRs.[76–79] Accordingly, to validate the functional implications of these findings, we subjected mECap18 cells to the highly selective pharmacological mTOR kinase inhibitor, everolimus,[48,80,81] with the timing of treatment selected to immediately precede that of the introduction of corticosterone at each media change (i.e., at 48 h intervals) throughout the 10-day exposure regimen (Figure 8A). mECap18 cells were then harvested in preparation for quantitative assessment of DNA damage using anti-γH2A.X antibodies; a sensitive marker of DNA double strand beaks. As illustrated in Figure 8B, minimal fluorescent foci of γH2A.X labeling were detected in the nuclei of vehicle control mECap18 cells. By comparison, and in keeping with pathway prediction analyses, mECap18 cells subjected to corticosterone treatment accrued a significant increase in γH2A.X labeling (both in terms of the number of labeled cells (Figure 8C) and the overall intensity of fluorescence (Figure 8D) indicative of an increase in the burden of DNA lesions (Figures 8B–D). Notably, however, the inclusion of everolimus supplementation in combination with corticosterone significantly attenuated γH2A.X labeling such that it was returned to basal levels indistinguishable from those detected in the mECap18 cells receiving vehicle only (Figures 8B–D).

4 | DISCUSSION

In what has now become a well described paradigm, spermatozoa are able to convey epigenetic stress signatures to perpetuate intergenerational, or perhaps even transgenerational, inheritance of a spectrum of paternal experiences to their offspring.[19,24,25,35,82–86] What remains less certain are the biological mechanisms by which paternal experiences alter the physiology of the epididymal epithelium to give rise to these intergenerational stress signals.[51] Here, we have a used

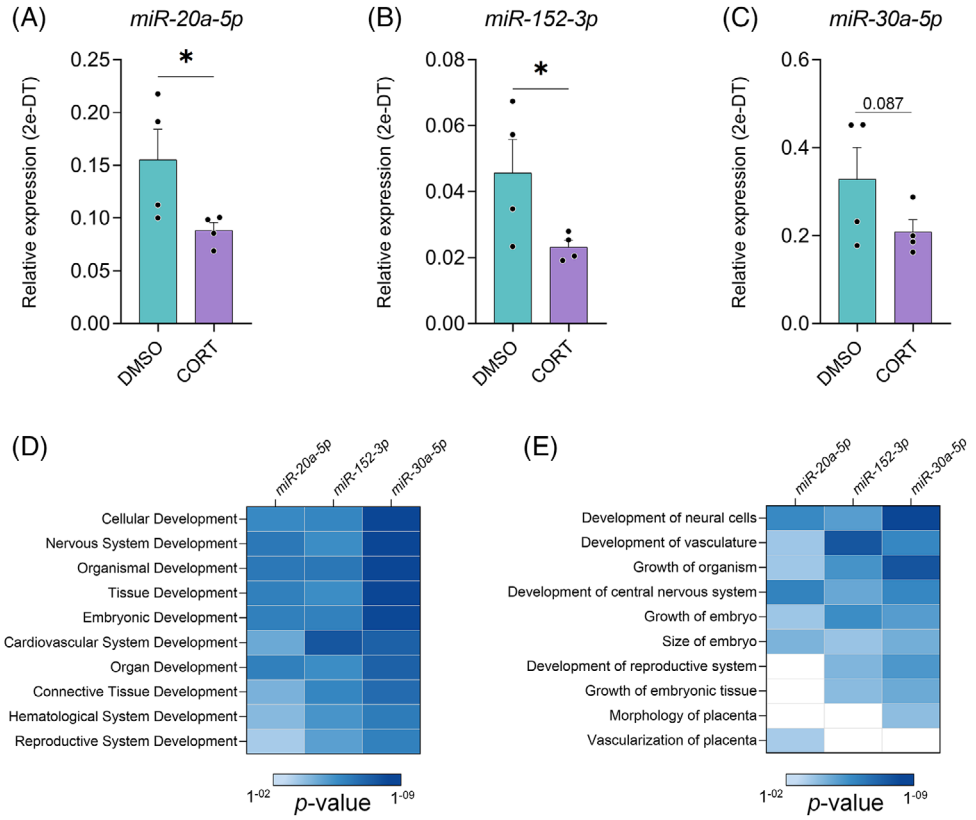

FIGURE 6 Corticosterone-induced miRNA changes in mECap18 cells. qPCR was used to determine the relative abundance of three target miRNAs in corticosterone challenged mECap18 cells. The relative expression of (A) *miR-20a-5p*, (B) *miR-152-3p*, and (C) *miR-30a-5p* normalized to a *U6snRNA* reference was calculated using the 2−ΔCt method. An unpaired *t*-test was applied to assess statistical significance of miRNA abundance in corticosterone challenged mECap18 cells (CORT) versus that of their vehicle only (DMSO) controls; * $p < 0.05$. Mean ± SEM ($n = 4$), with individual datapoints, are plotted in bar charts. Using the miRDB a list of predicted targets of each miRNA was obtained and submitted to IPA. Heatmaps depict comparative analyses of the top 10 most significant development related (D) networks and (E) functions across the three miRNAs.

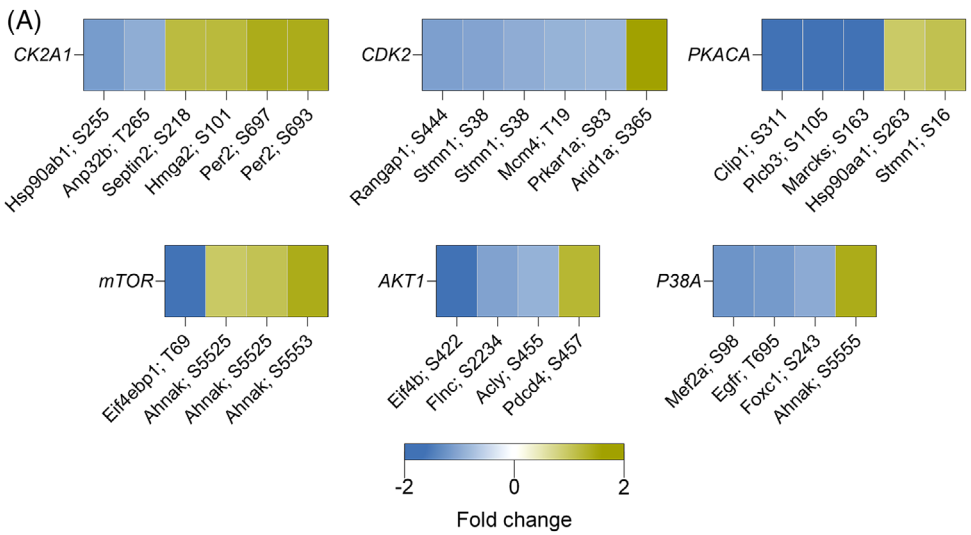

FIGURE 7 Kinase mapping to significantly altered phosphorylated residues. (A) Each kinase is represented as a heatmap with their substrates' fold change between vehicle and corticosteroid-treated samples indicated by color.

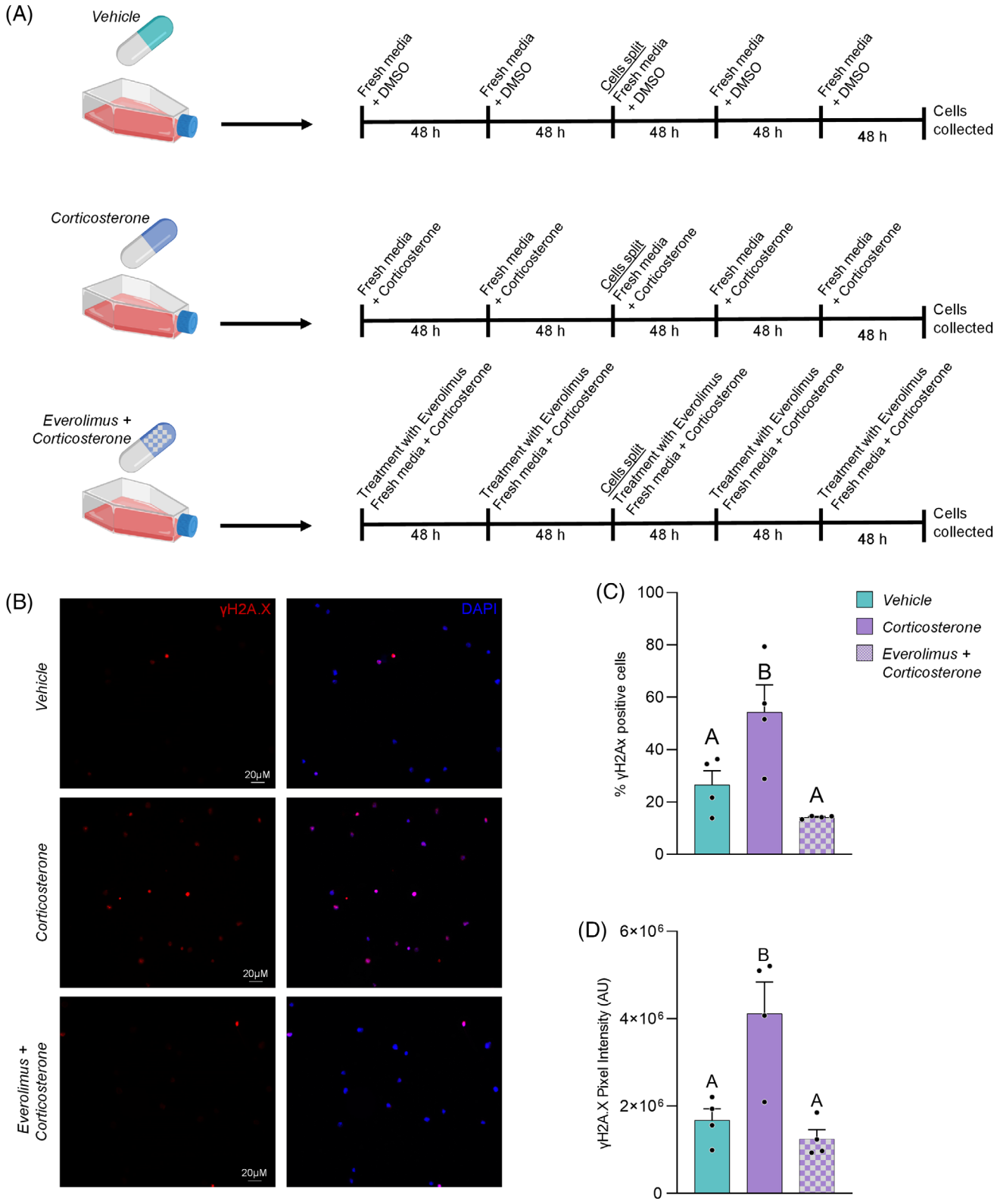

FIGURE 8 Selective pharmacological inhibition of mTOR reduces corticosterone-induced DNA damage. (A) Experimental design whereby mECap18 cells were exposed to either vehicle control (DMSO), 100 nM corticosterone, or 1 h pre-incubation with everolimus (mTOR inhibitor) prior to 100 nM corticosterone treatment. Replacement of media/treatments occurred at 48 h intervals over the course of a 10-day exposure regimen (B) After treatment, the level of DNA damage within mECap18 cells was measured by immunolabelling with anti-γH2A.X antibodies (red) and counterstained with DAPI (blue), to determine the number of (C) positively labeled cells and (D) the overall intensity of fluorescence in each cell population. A one-way ANOVA statistical test, with Tukey multiple correction, was applied to panels C and D. Mean ± SEM ($n = 4$), with individual datapoints, are plotted in bar charts.

phosphoproteomic strategy to characterize the molecular adaptation of mECap18 cells to corticosterone challenge. While the overall abundance of the majority of parent proteins was unchanged, the phosphorylation status of ~15% of all identified phosphoresidues were substantially modified in response to corticosterone stimulus. Notably, such changes were mapped to the putative activation of cellular stress response pathways, such as DDRs, chemokine signaling, and expression, transcription, and splicing of RNA. The former of these outcomes was orthogonally validated through immunodetection of an increased burden of DNA damage in corticosterone-treated cells and used to inform a successful amelioration strategy based on targeted inhibition of the mTOR kinase. Collectively, these data illustrate the utility of phosphoproteomics in predicting cellular responses to physiological relevant exogenous challenges and provide insight into pharmacological strategies with the potential to counter stress induced dysregulation of male reproduction.

To build our knowledge of how tissues of the male reproductive tract are innervated by paternal exposures, we elected to focus on direct administration of corticosterone, the primary glucocorticoid produced in mice,[87] and a hallmark of the hormonal response to stress. Indeed, numerous lifestyle and environmental stressors converge on the hypothalamic–pituitary–adrenal axis to drive adrenal gland synthesis and secretion of glucocorticoid hormones, including corticosterone. Upon release into circulation, corticosterone acts via canonical stress response pathways to prioritize survival (e.g., energy mobilization) over less essential physiological processes, before eventually eliciting an inhibitory negative-feedback loop, thereby limiting both the magnitude and duration of its influence.[88] In addition, corticosterone can also regulate a spectrum of alternate physiological processes, including growth and development, programmed cell death, immune/inflammatory responses, stress-related homeostasis, and reproduction.[89,90] The ability of corticosterone to induce such pleiotropic effects is determined, at least in part, by the relative abundance of its cognate receptor, nuclear receptor subfamily 3, group C, member 1 (NR3C1) within target tissues and cells.[91]

Rodent models of adrenal insufficiency have demonstrated that homeostatic levels of adrenal hormones, including glucocorticoids, are necessary for mediation of spermatogenesis, testicular steroidogenesis and, importantly in the context of this study, promoting sperm maturation.[92–94] However, despite this knowledge, and the conserved expression of NR3C1 among male reproductive tissues,[42] surprisingly little is known of the role of glucocorticoids in the male reproductive tract under normal physiological conditions nor how they drive the molecular adaptation of these tissues to stress. In terms of the epididymis, our study confirms that NR3C1 is differentially abundant along the length of the tract, with the highest levels of this protein documented in the proximal regions, coinciding with those segments in which the proteomic and epigenetic landscapes of the maturing spermatozoon are most dramatically altered.[13,14,18,22,23] This finding accords with independent evidence that the epididymis is under glucocorticoid regulation, with previous studies having implicated glucocorticoids in the absorptive and secretory activities of epididymal epithelial cells[95,96] as well as in zinc and copper metabolism within this tissue.[97,98] Our data also substantiate evidence that active NR3C1 is detected in a segment- and cell-specific pattern throughout the rat epididymis,[43] a model in which in vivo treatment with the synthetic glucocorticoid dexamethasone significantly alters the expression of glucocorticoid-responsive genes and induces NR3C1 nuclear translocation within the epididymal epithelial cells.[42] In extending these observations, the increased abundance of NR3C1 that ensues after chronic corticosterone challenge has been linked with an alteration to the protein and sncRNA cargo encapsulated within the extracellular vesicles produced by epididymal cell lines (DC2),[99] as well as downstream changes in the abundance of a subset of sperm miRNAs, and ultimately an altered offspring phenotype.[99,100] Consistent with such findings, here we confirmed that the abundance of a subset of stress-responsive miRNAs are altered in mECap18 cells in response to corticosterone challenge. Further, notwithstanding differences in the origin of the cell lines used across these studies (i.e., DC2 = distal caput vs. mECap18 = proximal caput epithelial cell lines), we noted conservation of 44% (i.e., 107 proteins) of the proteomic cargo identified in DC2 extracellular vesicles harvested after 4 days of corticosterone exposure, yet this overlap increased to 68% (i.e., 662 proteins) by day 11 post-treatment.[101] Together, these findings identify glucocorticoid/NR3C1 signaling as an additional tier of complexity to the interplay of known endocrine, paracrine, lumicrine, and neuronal systems that govern epididymal structure and function.

Such complex regulation has invariably limited advances in our understanding of epididymal physiology and the precise mechanisms through which this tissue exerts control over its luminal microenvironment and the population of maturing spermatozoa held therein.[8] The intricacies of these regulatory cascades might also go some way towards explaining the stark differences in the intergenerational responses recorded to varied experimental exposure regimens despite the imposition of similar durations of stress exposure.[102–104] In any case, such potential confounders identify the value of focusing on tractable cell culture systems to model the direct allostatic adaptation of the epididymis to external stressors prior to considering the spectrum of mitigating secondary influences that could influence its function in a stressed animal (e.g., age, physical status, prevailing environment, autonomic and sympathetic adaptations, and the timing of post-exposure matings). Accordingly, here, we have exploited cultured mECap18 cells, as we have previously done to deliver mechanistic insight into epididymal extracellular vesicle generation and secretion[46,72,105] as well as the response of this tissue to toxicant challenge.[106]

To our knowledge, this is the first study to apply advanced mass spectrometry strategies to establish broad scale proteomic inventory of the mECap18 epididymal epithelial cell line, in tandem with detailed analyses of the phosphorylation status of surveyed proteins, to model the allostatic adaptation of male reproductive tissues to exogenous stress. This strategy revealed pronounced changes to the phosphoproteome despite a relatively static overall proteomic response. Indeed, >99% of all identified proteins (4149) were represented in the core proteome of both vehicle control and corticosterone-treated mECap18 cells, with only a modest number of these proteins displaying

differential abundance under this imposed exposure regimen. Such subtle changes in mECap18 protein expression mirror that of the NR3C1 protein itself, the abundance of which was not substantially altered in response to corticosterone challenge. Based on these data, we speculate that NR3C1 may be subject to autoregulation to prevent excursions in abundance away from homeostatic levels; an adaptive response mirroring that recorded in other cell types.[107] Nevertheless, among the 73 proteins that were either uniquely detected or significantly altered in response to corticosterone challenge, we identified the putative activation of upstream stress response regulators, such as NRF2; itself considered a master transcription factor of an armada of genes involved in cellular defense.[108] Despite the growing number of pathological insults NRF2 has been linked to, its most widely documented role is that of a key regulator of antioxidant defenses.[109] It follows that "NRF2-mediated oxidative stress response" featured strongly among the cellular pathways identified by pathway analysis as being putatively activated in mECap18 cells subjected to corticosterone challenge. Together, these data support previous findings that elevated levels of glucocorticoid have the potential to induce oxidative stress in epididymal tissues[96]; thus raising the prospect that at least part of the molecular adaptation to corticosterone is directed toward mitigating the impact of oxidative lesions.

Consistent with this notion, pathway analysis of the 350 parent proteins identified as being differentially or uniquely phosphorylated in vehicle versus corticosterone-treated mECap18 cells revealed the putative activation of DDR pathways, and the related subcategories of BRCA1 DDR, ATM signaling and mismatch repair signaling; a finding commensurate with the increased DNA damage detected in corticosterone-treated mECap18 cells. Moreover, inhibition of mTOR, a known regulator of DNA damage,[110] significantly decreased the DNA damage burden in corticosterone-treated mECap18 cells to levels indistinguishable from those of control cells. Thus, alteration of the DDR represents a potential mechanism, orchestrated via NR3C1, via which paternal stressors can drive the biogenesis of "stressed" sncRNAs.[111,112] Accordingly, mapping of the biofunctions linked to the cohort of differentially phosphorylated proteins also revealed the predicted activation of "expression and transcription of DNA/RNA" as well as several categories associated with downstream "processing and splicing of RNA."

Such findings are in keeping with the recognized role of corticosterone engaging the master transcription factor, NR3C1.[91] However, the fact that this response was not linked to commensurate widespread increases in protein abundance among the global mECap18 proteome, raises the intriguing prospect that these pathways may target genes encoding regulatory, as opposed to protein coding, RNA species. Consistent with this notion, several regulators of sncRNA biosynthesis and processing were identified as being differentially phosphorylated following corticosterone challenge. Chief amongst these phosphorylated proteins was Smad nuclear-interacting protein 1 (SNIP1), an evolutionarily conserved factor involved in pre-mRNA splicing as a component of the spliceosome,[113] as well as a known interactor of the ribonuclease enzyme, DROSHA, which executes the initiation of pri-miRNA processing to form pre-miRNA.[31] The latter interaction implicates SNIP1 in regulating the biogenesis of several miRNAs including *let-7i*, *miR21*, *miR22*, *miR23*, and *miR25*.[114] These findings take on added significance in view of the fact that *let-7i* and *miR21* were identified among the top ranked differentially expressed miRNAs (log_2 fold change of ~1.8 for both) in the spermatozoa of corticosterone-treated mice[35]; suggesting that the phosphorylation, and hence activation, of SNIP1 may regulate the efficiency of corticosterone responsive miRNA precursor transcript processing and/or stability. Together, such findings allude to a putative mechanism that may, at least in part, account for how the epididymal epithelium responds to corticosterone as a prelude to relaying an altered profile of miRNAs to the male germline.

Nevertheless, additional proteins that experienced adaptive phosphorylation included the putative helicase MOV-10 (MOV10), which has an integral role in miRNA-mediated gene silencing, translational repression, and cleavage of complementary mRNAs.[115] Notably, MOV10 knockout mice have reduced proliferation of spermatogonial progenitor cells and reduced levels of miRNA synthesis in the testis,[116] yet to the best of our knowledge the implications of MOV10 loss have not been investigated in the context of post-testicular sperm maturation. Moreover, our data also identified increased phosphorylation of splicing factor 45, putative methyltransferase C9orf114 homolog and matrin-3, each of which have recently been implicated as part of the interactome of RNA-binding proteins that regulate miRNA biogenesis.[117] While further experimental evidence is clearly needed to substantiate the role that these proteins play in regulating epididymal responses to corticosterone, we and others have shown that the abundant sncRNA profile of epididymal epithelial cells[45] can be dynamically remodeled by diverse paternal stressors.[22,31] If this were to be the case, then our identification of a subset of kinases including CK2A1, CDK2, mTOR, and PKACA that drive corticosterone signaling cascades may offer druggable targets with which to counter stress induced alteration of male reproduction.

5 | CONCLUSION

In summary, here we have harnessed an advanced proteomic platform to define the impact of a direct corticosterone stimulus on cellular signaling pathways within a male reproductive cell line. This analysis revealed that, despite modest adaption of the global proteomic profile of the mECap18 lineage, corticosterone induced pronounced changes across the phosphoproteome of these cells. Interrogation of these phosphorylation events identified the important interplay of DNA damage and associated repair pathways as being among those most heavily affected by the adaptation to the imposed corticosterone challenge. These data provide new insight into the repercussions of exogenous stressors on epididymal function and male fertility more broadly.

AUTHOR CONTRIBUTIONS

Conceptualization: D. A. S. B. and B. N. *Methodology*: D. A. S. B., S. J. S., N. A. T., A. L. A., I. R. B., T. L., J. E. S., H. C. M., N. M. V., and B. N. *Investigation*: D. A. S. B., S. J. S., N. A. T., A. L. A., I. R. B., and J. E. S. *Formal analysis*: D.

A. S. B., I. R. B., J. E. S., and B. N. *Validation*: D. A. S. B., S. J. S., N. A. T., A. L. A., I. R. B., J. E. S. *Writing—original draft*: D. A. S. B. and B. N. *Writing—review and editing*: D. A. S. B., S. J. S., N. A. T., A. L. A., P. S., I. R. B., T. L., J. E. S., H. C. M., N. M. V., M. D. D., T. Y. P., and B. N. *Funding acquisition*: B. N. and M. D. D. *Resources*: P. S., T. L., H. C. M., N. V. M., and B. N. *Supervision*: B. N.

ACKNOWLEDGMENTS

We thank Nathan Smith from The University of Newcastle Analytical Biomolecular Research Facility (ABRF), and the Academic and Research Computing Support team at The University of Newcastle who provided High Performance Computing Infrastructure to support the bioinformatics analyses. The preparation of this manuscript was supported by the award of National Health and Medical Research Council (NHMRC) Project Grants APP1147932, awarded to B. N. and M. D. D. B. N. (APP1154837) and M. D. D. (APP1173892) are recipients of NHMRC Research Fellowships. M. D. D. is also supported by Defeat DIPG ChadTough New Investigator Fellowship.

CONFLICT OF INTEREST STATEMENT

The authors declare that they have no conflicts of interest.

DATA AVAILABILITY STATEMENT

The mass spectrometry proteomics data have been deposited to the ProteomeXchange Consortium (http://proteomecentral.proteomexchange.org) via the PRIDE partner repository[118] with the dataset identifier PXD028789 and https://doi.org/10.6019/PXD028789.

ORCID

David A. Skerrett-Byrne https://orcid.org/0000-0002-1804-1826
Brett Nixon https://orcid.org/0000-0003-2745-8188

REFERENCES

1. Bedford JM. Effects of duct ligation on the fertilizing ability of spermatozoa from different regions of the rabbit epididymis. *J Exp Zool*. 1967;166(2):271-281. doi:10.1002/jez.1401660210
2. Orgebin-Crist MC. Sperm maturation in rabbit epididymis. *Nature*. 1967;216(5117):816-818. doi:10.1038/216816a0
3. Orgebin-Crist MC. Maturation of spermatozoa in the rabbit epididymis: delayed fertilization in does inseminated with epididymal spermatozoa. *J Reprod Fertil*. 1968;16(1):29-33. doi:10.1530/jrf.0.0160029
4. Orgebin-Crist MC. Studies on the function of the epididymis. *Biol Reprod*. 1969;1(1):155-175. doi:10.1095/biolreprod1.supplement_1.155. Suppl.
5. Bedford JM. Components of sperm maturation in the human epididymis. *Adv Biosci*. 1973;10:145-155.
6. Bedford JM. Enigmas of mammalian gamete form and function. *Biol Rev Camb Philos Soc*. 2004;79(2):429-460. doi:10.1017/s146479310300633x
7. Bedford JM. The epididymis re-visited: a personal view. *Asian J Androl*. 2015;17(5):693-698. doi:10.4103/1008-682X.153297
8. Nixon B, Cafe SL, Eamens AL, et al. Molecular insights into the divergence and diversity of post-testicular maturation strategies. *Mol Cell Endocrinol*. 2020;517:110955. doi:10.1016/j.mce.2020.110955
9. Bedford JM. Singular features of fertilization and their impact on the male reproductive system in eutherian mammals. *Reproduction*. 2014;147(2):R43-52. doi:10.1530/REP-13-0436
10. Zhou W, De Iuliis GN, Dun MD, Nixon B. Characteristics of the epididymal luminal environment responsible for sperm maturation and storage. *Front Endocrinol (Lausanne)*. 2018;9:59. doi:10.3389/fendo.2018.00059
11. Dacheux JL, Dacheux F, Druart X. Epididymal protein markers and fertility. *Anim Reprod Sci*. 2016;169:76-87. doi:10.1016/j.anireprosci.2016.02.034
12. Dacheux JL, Dacheux F. New insights into epididymal function in relation to sperm maturation. *Reproduction*. 2014;147(2):R27-42. doi:10.1530/REP-13-0420
13. Dacheux JL, Belleannee C, Guyonnet B, et al. The contribution of proteomics to understanding epididymal maturation of mammalian spermatozoa. *Syst Biol Reprod Med*. 2012;58(4):197-210. doi:10.3109/19396368.2012.663233
14. Dacheux JL, Belleannee C, Jones R, et al. Mammalian epididymal proteome. *Mol Cell Endocrinol*. 2009;306(1-2):45-50. doi:10.1016/j.mce.2009.03.007
15. Aitken RJ, Nixon B, Lin M, Koppers AJ, Lee YH, Baker MA. Proteomic changes in mammalian spermatozoa during epididymal maturation. *Asian J Androl*. 2007;9(4):554-564. doi:10.1111/j.1745-7262.2007.00280.x
16. Dacheux JL, Gatti JL, Dacheux F. Contribution of epididymal secretory proteins for spermatozoa maturation. *Microsc Res Tech*. 2003;61(1):7-17. doi:10.1002/jemt.10312
17. Skerget S, Rosenow MA, Petritis K, Karr TL. Sperm proteome maturation in the mouse epididymis. *PLoS One*. 2015;10(11):e0140650. doi:10.1371/journal.pone.0140650
18. Skerrett-Byrne DA, Anderson AL, Bromfield EG, et al. Global profiling of the proteomic changes associated with the post-testicular maturation of mouse spermatozoa. *Cell Reports*. 2022;41(7):111655.
19. Conine CC, Sun F, Song L, Rivera-Perez JA, Rando OJ. Small RNAs gained during epididymal transit of sperm are essential for embryonic development in mice. *Dev Cell*. 2018;46(4):470-480. doi:10.1016/j.devcel.2018.06.024. e3.
20. Conine CC, Sun F, Song L, Rivera-Perez JA, Rando OJ. MicroRNAs absent in caput sperm are required for normal embryonic development. *Dev Cell*. 2019;50(1):7-8. doi:10.1016/j.devcel.2019.06.007
21. Hutcheon K, McLaughlin EA, Stanger SJ, et al. Analysis of the small non-protein-coding RNA profile of mouse spermatozoa reveals specific enrichment of piRNAs within mature spermatozoa. *RNA Biol*. 2017;14(12):1776-1790. doi:10.1080/15476286.2017.1356569
22. Nixon B, De Iuliis GN, Dun MD, Zhou W, Trigg NA, Eamens AL. Profiling of epididymal small non-protein-coding RNAs. *Andrology*. 2019;7(5):669-680. doi:10.1111/andr.12640
23. Nixon B, Stanger SJ, Mihalas BP, et al. The microRNA signature of mouse spermatozoa is substantially modified during epididymal maturation. *Biol Reprod*. 2015;93(4):91. doi:10.1095/biolreprod.115.132209
24. Sharma U, Conine CC, Shea JM, et al. Biogenesis and function of tRNA fragments during sperm maturation and fertilization in mammals. *Science*. 2016;351(6271):391-396. doi:10.1126/science.aad6780
25. Sharma U, Sun F, Conine CC, et al. Small RNAs Are trafficked from the epididymis to developing mammalian sperm. *Dev Cell*. 2018;46(4):481-494. doi:10.1016/j.devcel.2018.06.023. e6.
26. Nixon B, De Iuliis GN, Hart HM, et al. Proteomic profiling of mouse epididymosomes reveals their contributions to post-testicular sperm maturation. *Mol Cell Proteomics*. 2019;18(1):S91-s108. doi:10.1074/mcp.RA118.000946. Suppl.
27. Zhou W, Stanger SJ, Anderson AL, et al. Mechanisms of tethering and cargo transfer during epididymosome-sperm interactions. *BMC Biol*. 2019;17(1):35. doi:10.1186/s12915-019-0653-5

28. Reilly JN, McLaughlin EA, Stanger SJ, et al. Characterisation of mouse epididymosomes reveals a complex profile of microRNAs and a potential mechanism for modification of the sperm epigenome. *Sci Rep*. 2016;6:31794. doi:10.1038/srep31794
29. Trigg NA, Skerrett-Byrne DA, Xavier MJ, et al. Acrylamide modulates the mouse epididymal proteome to drive alterations in the sperm small non-coding RNA profile and dysregulate embryo development. *Cell Rep*. 2021;37(1):109787. doi:10.1016/j.celrep.2021.109787
30. Yin X, Anwar A, Wang Y, Hu H, Liang G, Zhang C. Paternal environmental exposure-induced spermatozoal small noncoding RNA alteration meditates the intergenerational epigenetic inheritance of multiple diseases. *Front Med*. 2022;16(2):176-184. doi:10.1007/s11684-021-0885-y
31. Trigg NA, Eamens AL, Nixon B. The contribution of epididymosomes to the sperm small RNA profile. *Reproduction*. 2019;157(6):R209-r223. doi:10.1530/rep-18-0480
32. Nätt D, Öst A. Male reproductive health and intergenerational metabolic responses from a small RNA perspective. *J Intern Med*. 2020;288(3):305-320. doi:10.1111/joim.13096
33. Ly L, Chan D, Trasler JM. Developmental windows of susceptibility for epigenetic inheritance through the male germline. *Semin Cell Dev Biol*. 2015;43:96-105. doi:10.1016/j.semcdb.2015.07.006
34. Klastrup LK, Bak ST, Nielsen AL. The influence of paternal diet on sncRNA-mediated epigenetic inheritance. *Mol Genet Genomics*. 2019;294(1):1-11. doi:10.1007/s00438-018-1492-8
35. Short AK, Fennell KA, Perreau VM, et al. Elevated paternal glucocorticoid exposure alters the small noncoding RNA profile in sperm and modifies anxiety and depressive phenotypes in the offspring. *Transl Psychiatry*. 2016;6(6):e837. doi:10.1038/tp.2016.109
36. Rawat A, Guo J, Renoir T, Pang TY, Hannan AJ. Hypersensitivity to sertraline in the absence of hippocampal 5-HT1AR and 5-HTT gene expression changes following paternal corticosterone treatment. *Environ Epigenet*. 2018;4(2):dvy015. doi:10.1093/eep/dvy015
37. Ihne JL, Fitzgerald PJ, Hefner KR, Holmes A. Pharmacological modulation of stress-induced behavioral changes in the light/dark exploration test in male C57BL/6J mice. *Neuropharmacology*. 2012;62(1):464-473. doi:10.1016/j.neuropharm.2011.08.045
38. Mozhui K, Karlsson RM, Kash TL, et al. Strain differences in stress responsivity are associated with divergent amygdala gene expression and glutamate-mediated neuronal excitability. *J Neurosci*. 2010;30(15):5357-5367. doi:10.1523/JNEUROSCI.5017-09.2010
39. Wu L, Lu Y, Jiao Y, et al. Paternal psychological stress reprograms hepatic gluconeogenesis in offspring. *Cell Metab*. 2016;23(4):735-743. doi:10.1016/j.cmet.2016.01.014
40. Motavalli R, Majidi T, Pourlak T, et al. The clinical significance of the glucocorticoid receptors: genetics and epigenetics. *J Steroid Biochem Mol Biol*. 2021;213:105952. doi:10.1016/j.jsbmb.2021.105952
41. Silva EJ, Queiroz DB, Rodrigues A, Honda L, Avellar MC. Innate immunity and glucocorticoids: potential regulatory mechanisms in epididymal biology. *J Androl*. 2011;32(6):614-624. doi:10.2164/jandrol.111.013565
42. Silva EJ, Queiroz DB, Honda L, Avellar MC. Glucocorticoid receptor in the rat epididymis: expression, cellular distribution and regulation by steroid hormones. *Mol Cell Endocrinol*. 2010;325(1-2):64-77. doi:10.1016/j.mce.2010.05.013
43. Schultz R, Isola J, Parvinen M, et al. Localization of the glucocorticoid receptor in testis and accessory sexual organs of male rat. *Mol Cell Endocrinol*. 1993;95(1-2):115-120. doi:10.1016/0303-7207(93)90036-j
44. Sipila P, Shariatmadari R, Huhtaniemi IT, Poutanen M. Immortalization of epididymal epithelium in transgenic mice expressing simian virus 40 T antigen: characterization of cell lines and regulation of the polyoma enhancer activator 3. *Endocrinology*. 2004;145(1):437-446. doi:10.1210/en.2003-0831
45. Nixon B, Stanger SJ, Mihalas BP, et al. Next generation sequencing analysis reveals segmental patterns of microRNA expression in mouse epididymal epithelial cells. *PLoS One*. 2015;10(8):e0135605. doi:10.1371/journal.pone.0135605
46. Zhou W, Sipila P, De Iuliis GN, Dun MD, Nixon B. Analysis of epididymal protein synthesis and secretion. *J Vis Exp*. 2018;138:e58308. doi:10.3791/58308
47. Fennell KA, Busby RGG, Li S, et al. Limitations to intergenerational inheritance: subchronic paternal stress preconception does not influence offspring anxiety. *Sci Rep*. 2020;10(1):16050. doi:10.1038/s41598-020-72560-z
48. Owonikoko TK, Zhang G, Lallani SB, et al. Evaluation of preclinical efficacy of everolimus and pasireotide in thyroid cancer cell lines and xenograft models. *PLoS One*. 2019;14(2):e0206309. doi:10.1371/journal.pone.0206309
49. Laemmli UK. Cleavage of structural proteins during the assembly of the head of bacteriophage T4. *Nature*. 1970;227:680-685.
50. Towbin H, Staehelin T, Gordon J. Electrophoretic transfer of proteins from polyacrylamide gels to nitrocellulose sheets: procedure and some applications. *Proc Natl Acad Sci USA*. 1979;76(9):4350-4354.
51. Trigg NA, Skerrett-Byrne DA, Xavier MJ, et al. Acrylamide modulates the mouse epididymal proteome to drive alterations in the sperm small non-coding RNA profile and dysregulate embryo development. *Cell Rep*. 2021;37:109787.
52. Schmittgen TD, Livak KJ. Analyzing real-time PCR data by the comparative C(T) method. *Nat Protoc*. 2008;3(6):1101-1108. doi:10.1038/nprot.2008.73
53. Schjenken JE, Moldenhauer LM, Zhang B, et al. MicroRNA miR-155 is required for expansion of regulatory T cells to mediate robust pregnancy tolerance in mice. *Mucosal Immunol*. 2020;13(4):609-625. doi:10.1038/s41385-020-0255-0
54. Humphrey SJ, Karayel O, James DE, Mann M. High-throughput and high-sensitivity phosphoproteomics with the EasyPhos platform. *Nat Protoc*. 2018;13(9):1897-1916. doi:10.1038/s41596-018-0014-9
55. Smyth SP, Nixon B, Anderson AL, et al. Elucidation of the protein composition of mouse seminal vesicle fluid. *Proteomics*. 2022;22(9):e2100227. doi:10.1002/pmic.202100227
56. Rappsilber J, Mann M, Ishihama Y. Protocol for micro-purification, enrichment, pre-fractionation and storage of peptides for proteomics using StageTips. *Nat Protoc*. 2007;2(8):1896-1906. doi:10.1038/nprot.2007.261
57. Degryse S, de Bock CE, Demeyer S, et al. Mutant JAK3 phosphoproteomic profiling predicts synergism between JAK3 inhibitors and MEK/BCL2 inhibitors for the treatment of T-cell acute lymphoblastic leukemia. *Leukemia*. 2018;32(3):788-800. doi:10.1038/leu.2017.276
58. Murray HC, Enjeti AK, Kahl RGS, et al. Quantitative phosphoproteomics uncovers synergy between DNA-PK and FLT3 inhibitors in acute myeloid leukaemia. *Leukemia*. 2021;35(6):1782-1787. doi:10.1038/s41375-020-01050-y
59. Nixon B, Johnston SD, Skerrett-Byrne DA, et al. Modification of crocodile spermatozoa refutes the tenet that post-testicular sperm maturation is restricted to mammals. *Mol Cell Proteomics*. 2019;18(1):S58-s76. doi:10.1074/mcp.RA118.000904. Suppl.
60. Skerrett-Byrne DA, Bromfield EG, Murray HC, et al. Time-resolved proteomic profiling of cigarette smoke-induced experimental chronic obstructive pulmonary disease. *Respirology*. 2021;26:960-973. doi:10.1111/resp.14111
61. Skerrett-Byrne DA, Trigg NA, Bromfield EG, et al. Proteomic dissection of the impact of environmental exposures on mouse seminal vesicle function. *Mol Cell Proteomics*. 2021;20:100107. doi:10.1016/j.mcpro.2021.100107
62. Taus T, Köcher T, Pichler P, et al. Universal and confident phosphorylation site localization using phosphoRS. *J Proteome Res*. 2011;10(12):5354-5362. doi:10.1021/pr200611n

63. Tyanova S, Temu T, Sinitcyn P, et al. The Perseus computational platform for comprehensive analysis of (prote)omics data. *Nat Methods*. 2016;13(9):731-740. doi:10.1038/nmeth.3901
64. Skerrett-Byrne DA, Anderson AL, Hulse L, et al. Proteomic analysis of koala (Phascolarctos cinereus) spermatozoa and prostatic bodies. *Proteomics*. 2021;21(19):e2100067. doi:10.1002/pmic.202100067
65. Zhang M, Chiozzi RZ, Skerrett-Byrne DA, et al. High resolution proteomic analysis of subcellular fractionated boar spermatozoa provides comprehensive insights into perinuclear theca-residing proteins. *Front Cell Dev Biol*. 2022;10:836208. doi:10.3389/fcell.2022.836208
66. Skerrett-Byrne DA, Nixon B, Bromfield EG, et al. Transcriptomic analysis of the seminal vesicle response to the reproductive toxicant acrylamide. *BMC Genomics*. 2021;22(1):728. doi:10.1186/s12864-021-07951-1
67. Krämer A, Green J, Pollard J Jr, Tugendreich S. Causal analysis approaches in ingenuity pathway analysis. *Bioinformatics*. 2014;30(4):523-530. doi:10.1093/bioinformatics/btt703
68. Chen Y, Wang X. miRDB: an online database for prediction of functional microRNA targets. *Nucleic Acids Res*. 2020;48(D1):D127-D131.
69. Liu W, Wang X. Prediction of functional microRNA targets by integrative modeling of microRNA binding and target expression data. *Genome Biol*. 2019;20:1-10.
70. Hornbeck PV, Zhang B, Murray B, Kornhauser JM, Latham V, Skrzypek E. PhosphoSitePlus, 2014: mutations, PTMs and recalibrations. *Nucleic Acids Res*. 2015;43:D512-520. doi:10.1093/nar/gku1267. Database issue.
71. Johnston DS, Jelinsky SA, Bang HJ, et al. The mouse epididymal transcriptome: transcriptional profiling of segmental gene expression in the epididymis. *Biol Reprod*. 2005;73(3):404-413. doi:10.1095/biolreprod.105.039719
72. Trigg NA, Stanger SJ, Zhou W, et al. A novel role for milk fat globule-EGF factor 8 protein (MFGE8) in the mediation of mouse sperm-extracellular vesicle interactions. *Proteomics*. 2021;21(13-14):e2000079. doi:10.1002/pmic.202000079
73. Mulhall JE, Trigg NA, Bernstein IR, et al. Immortalized mouse caput epididymal epithelial (mECap18) cell line recapitulates the in-vivo environment. *Proteomics*. 2023:e2300253. doi:10.1002/pmic.202300253
74. Cortez D, Wang Y, Qin J, Elledge SJ. Requirement of ATM-dependent phosphorylation of brca1 in the DNA damage response to double-strand breaks. *Science*. 1999;286(5442):1162-1166. doi:10.1126/science.286.5442.1162
75. Pearl LH, Schierz AC, Ward SE, Al-Lazikani B, Pearl FM. Therapeutic opportunities within the DNA damage response. *Nat Rev Cancer*. 2015;15(3):166-180. doi:10.1038/nrc3891
76. Wang H, Kim NH. CDK2 is required for the DNA damage response during porcine early embryonic development. *Biol Reprod*. 2016;95(2):31. doi:10.1095/biolreprod.116.140244
77. Liberal V, Martinsson-Ahlzén HS, Liberal J, et al. Cyclin-dependent kinase subunit (Cks) 1 or Cks2 overexpression overrides the DNA damage response barrier triggered by activated oncoproteins. *Proc Natl Acad Sci USA*. 2012;109(8):2754-2759. doi:10.1073/pnas.1102434108
78. Phong MS, Van Horn RD, Li S, Tucker-Kellogg G, Surana U, Ye XS. p38 mitogen-activated protein kinase promotes cell survival in response to DNA damage but is not required for the G(2) DNA damage checkpoint in human cancer cells. *Mol Cell Biol*. 2010;30(15):3816-3826. doi:10.1128/mcb.00949-09
79. Liu Q, Turner KM, Alfred Yung WK, Chen K, Zhang W. Role of AKT signaling in DNA repair and clinical response to cancer therapy. *Neuro Oncol*. 2014;16(10):1313-1323. doi:10.1093/neuonc/nou058
80. Ma Y, Vassetzky Y, Dokudovskaya S. mTORC1 pathway in DNA damage response. *Biochim Biophys Acta Mol Cell Res*. 2018;1865(9):1293-1311. doi:10.1016/j.bbamcr.2018.06.011
81. Findlay IJ, De Iuliis GN, Duchatel RJ, et al. Pharmaco-proteogenomic profiling of pediatric diffuse midline glioma to inform future treatment strategies. *Oncogene*. 2022;41(4):461-475. doi:10.1038/s41388-021-02102-y
82. Chan JC, Nugent BM, Bale TL. Parental advisory: maternal and paternal stress can impact offspring neurodevelopment. *Biol Psychiatry*. 2018;83(10):886-894. doi:10.1016/j.biopsych.2017.10.005
83. Chen Q, Yan W, Duan E. Epigenetic inheritance of acquired traits through sperm RNAs and sperm RNA modifications. *Nat Rev Genet*. 2016;17(12):733-743. doi:10.1038/nrg.2016.106
84. Pang TYC, Short AK, Bredy TW, Hannan AJ. Transgenerational paternal transmission of acquired traits: stress-induced modification of the sperm regulatory transcriptome and offspring phenotypes. *Curr Opin Behav Sci*. 2017;14:140-147. doi:10.1016/j.cobeha.2017.02.007
85. Sharma U. Paternal contributions to offspring health: role of sperm small RNAs in intergenerational transmission of epigenetic information. *Front Cell Dev Biol*. 2019;7:215. doi:10.3389/fcell.2019.00215
86. Short AK, Yeshurun S, Powell R, et al. Exercise alters mouse sperm small noncoding RNAs and induces a transgenerational modification of male offspring conditioned fear and anxiety. *Transl Psychiatry*. 2017;7(5):e1114. doi:10.1038/tp.2017.82
87. Auchus RJ. Steroid 17-hydroxylase and 17,20-lyase deficiencies, genetic and pharmacologic. *J Steroid Biochem Mol Biol*. 2017;165:71-78. doi:10.1016/j.jsbmb.2016.02.002. Pt A.
88. Oyola MG, Handa RJ. Hypothalamic-pituitary-adrenal and hypothalamic-pituitary-gonadal axes: sex differences in regulation of stress responsivity. *Stress*. 2017;20(5):476-494. doi:10.1080/10253890.2017.1369523
89. Cooke PS, Holsberger DR, Witorsch RJ, et al. Thyroid hormone, glucocorticoids, and prolactin at the nexus of physiology, reproduction, and toxicology. *Toxicol Appl Pharmacol*. 2004;194(3):309-335. doi:10.1016/j.taap.2003.09.016
90. Zhou J, Cidlowski JA. The human glucocorticoid receptor: one gene, multiple proteins and diverse responses. *Steroids*. 2005;70(5-7):407-417. doi:10.1016/j.steroids.2005.02.006
91. Kumar R, Thompson EB. Gene regulation by the glucocorticoid receptor: structure:function relationship. *J Steroid Biochem Mol Biol*. 2005;94(5):383-394. doi:10.1016/j.jsbmb.2004.12.046
92. Weber MA, Groos S, Hopfl U, Spielmann M, Aumuller G, Konrad L. Glucocorticoid receptor distribution in rat testis during postnatal development and effects of dexamethasone on immature peritubular cells in vitro. *Andrologia*. 2000;32(1):23-30.
93. Lescoat G, Lescoat D, Garnier DH. Influence of adrenalectomy on maturation of gonadotrophin function in the male rat. *J Endocrinol*. 1982;95(1):1-6. doi:10.1677/joe.0.0950001
94. Gao HB, Ge RS, Lakshmi V, Marandici A, Hardy MP. Hormonal regulation of oxidative and reductive activities of 11 beta-hydroxysteroid dehydrogenase in rat Leydig cells. *Endocrinology*. 1997;138(1):156-161. doi:10.1210/endo.138.1.4837
95. Au CL, Ngai HK, Yeung CH, Wong PY. Effect of adrenalectomy and hormone replacement on sodium and water transport in the perfused rat cauda epididymidis. *J Endocrinol*. 1978;77(2):265-266. doi:10.1677/joe.0.0770265
96. Garcia-Diaz EC, Gomez-Quiroz LE, Arenas-Rios E, Aragon-Martinez A, Ibarra-Arias JA, del Socorro IR-MM. Oxidative status in testis and epididymal sperm parameters after acute and chronic stress by cold-water immersion in the adult rat. *Syst Biol Reprod Med*. 2015;61(3):150-160. doi:10.3109/19396368.2015.1008071
97. Nair N, Bedwal RS, Mathur RS. Zinc, copper and hydrolytic enzymes in epididymis of hydrocortisone treated rat. *Indian J Exp Biol*. 1998;36(1):22-33.
98. Nair N, Bedwal RS, Mathur RS. Effect of adrenalectomy on rat epididymidis. *Asian J Androl*. 2002;4(4):273-279.
99. Chan JC, Morgan CP, Adrian Leu N, et al. Reproductive tract extracellular vesicles are sufficient to transmit intergenerational stress and

program neurodevelopment. *Nat Commun*. 2020;11(1):1499. doi:10.1038/s41467-020-15305-w
100. Chan JC, Nugent BM, Morrison KE, et al. Epididymal glucocorticoid receptors promote intergenerational transmission of paternal stress. *bioRxiv*. 2018:321976. doi:10.1101/321976
101. Chan JC, Morgan CP, Adrian Leu N, et al. Reproductive tract extracellular vesicles are sufficient to transmit intergenerational stress and program neurodevelopment. *Nat Commun*. 2020;11(1):1499. doi:10.1038/s41467-020-15305-w
102. Harris AZ, Atsak P, Bretton ZH, et al. A novel method for chronic social defeat stress in female mice. *Neuropsychopharmacology*. 2018;43(6):1276-1283. doi:10.1038/npp.2017.259
103. Nakatake Y, Furuie H, Yamada M, et al. The effects of emotional stress are not identical to those of physical stress in mouse model of social defeat stress. *Neurosci Res*. 2020;158:56-63. doi:10.1016/j.neures.2019.10.008
104. Menard C, Pfau ML, Hodes GE, et al. Social stress induces neurovascular pathology promoting depression. *Nat Neurosci*. 2017;20(12):1752-1760. doi:10.1038/s41593-017-0010-3
105. Zhou W, De Iuliis GN, Turner AP, et al. Developmental expression of the dynamin family of mechanoenzymes in the mouse epididymis. *Biol Reprod*. 2017;96(1):159-173. doi:10.1095/biolreprod.116.145433
106. Katen AL, Sipila P, Mitchell LA, Stanger SJ, Nixon B, Roman SD. Epididymal CYP2E1 plays a critical role in acrylamide-induced DNA damage in spermatozoa and paternally mediated embryonic resorptions. *Biol Reprod*. 2017;96(4):921-935. doi:10.1093/biolre/iox021
107. Burnstein KL, Bellingham DL, Jewell CM, Powell-Oliver FE, Cidlowski JA. Autoregulation of glucocorticoid receptor gene expression. *Steroids*. 1991;56(2):52-58. doi:10.1016/0039-128x(91)90124-e
108. Zang H, Mathew RO, Cui T. The dark side of Nrf2 in the heart. *Front Physiol*. 2020;11:722. doi:10.3389/fphys.2020.00722
109. Nguyen T, Nioi P, Pickett CB. The Nrf2-antioxidant response element signaling pathway and its activation by oxidative stress. *J Biol Chem*. 2009;284(20):13291-13295. doi:10.1074/jbc.R900010200
110. Krieger KL, Hu WF, Ripperger T, Woods NT. Functional impacts of the BRCA1-mTORC2 interaction in breast cancer. *Int J Mol Sci*. 2019;20(23):5876. doi:10.3390/ijms20235876
111. di Fagagna FDA. A direct role for small non-coding RNAs in DNA damage response. *Trends Cell Biol*. 2014;24(3):171-178.
112. Wei W, Ba Z, Gao M, et al. A role for small RNAs in DNA double-strand break repair. *Cell*. 2012;149(1):101-112. doi:10.1016/j.cell.2012.03.002
113. Zhang X, Yan C, Zhan X, Li L, Lei J, Shi Y. Structure of the human activated spliceosome in three conformational states. *Cell Res*. 2018;28(3):307-322. doi:10.1038/cr.2018.14
114. Yu B, Bi L, Zheng B, et al. The FHA domain proteins DAWDLE in Arabidopsis and SNIP1 in humans act in small RNA biogenesis. *Proc Natl Acad Sci USA*. 2008;105(29):10073-10078. doi:10.1073/pnas.0804218105
115. Nawaz A, Shilikbay T, Skariah G, Ceman S. Unwinding the roles of RNA helicase MOV10. *Wiley Interdiscip Rev RNA*. 2021;13:e1682. doi:10.1002/wrna.1682
116. Frost RJ, Hamra FK, Richardson JA, Qi X, Bassel-Duby R, Olson EN. MOV10L1 is necessary for protection of spermatocytes against retrotransposons by Piwi-interacting RNAs. *Proc Natl Acad Sci USA*. 2010;107(26):11847-11852. doi:10.1073/pnas.1007158107
117. Treiber T, Treiber N, Plessmann U, et al. A compendium of RNA-binding proteins that regulate microRNA biogenesis. *Mol Cell*. 2017;66(2):270-284. doi:10.1016/j.molcel.2017.03.014. e13.
118. Perez-Riverol Y, Csordas A, Bai J, et al. The PRIDE database and related tools and resources in 2019: improving support for quantification data. *Nucleic Acids Res*. 2019;47(D1):D442-d450. doi:10.1093/nar/gky1106

SUPPORTING INFORMATION

Additional supporting information can be found online in the Supporting Information section at the end of this article.

How to cite this article: Skerrett-Byrne DA, Stanger SJ, Trigg NA, et al. Phosphoproteomic analysis of the adaption of epididymal epithelial cells to corticosterone challenge. *Andrology*. 2024;1-20. https://doi.org/10.1111/andr.13636